Code 2020

NRL REPORT 3565

COPY NO.

FR-3565

AN I-F SIGNAL SIMULATOR FOR MONOPULSE RADARS

NAVAL RESEARCH LABORATORY

WASHINGTON, D.C.

NRL REPORT 3565

AN I-F SIGNAL SIMULATOR FOR MONOPULSE RADARS

A. M. King

April 29, 1949

Approved by:

J. E. Meade, Head, Radar I Branch
R. M. Page, Superintendent, Radio Division III

NAVAL RESEARCH LABORATORY
CAPTAIN F. R. FURTH, USN, DIRECTOR
WASHINGTON, D.C.

CONTENTS

DISTRIBUTION

CNO	1
BuOrd	
Attn: Code Re4f	5
Attn: Code Re4c	5
Dir., USNEL	2
CDR, USNOTS	
Attn: Reports Unit	2
BAGR, CD, Wright-Patterson AFB	
Attn: CADO-D1	1
ONR	
Attn: Code 470	1
Supt., USNPGS	1
CG, AMC, Wright-Patterson AFB	
Attn: Eng. Div., Electronics Subdiv., MCREEO-2	1
CO, Watson Labs., AMC, Red Bank	
Attn: ENR	1
CO, Air Force Cambridge Res. Labs.	
Attn: ERRS	1
RDB	
Attn: Library	2
Attn: Navy Secretary	1
Naval Res. Sec., Science Div., Library of Congress	
Attn: Mr. J. H. Heald	2
ANAF/GM Mailing List No. 9	
Parts A, C, and DG	167

ABSTRACT

The development of i-f amplifiers for use in the TAB radar system requires controlled adjustment and accurate measurement of phase angles at the radar i-f. An i-f signal simulator has been developed capable of establishing or measuring phase angles with a calibrated accuracy of $\pm 2^{\circ}$, or $\pm$ 2.5 percent of the involved angle, whichever figure is the smaller. A phase sensitivity of 0.1° is realized. This performance is obtained by means of a calibrated 360° phase-shift condenser.

Design considerations are discussed, and experimental performance analyzed and compared with theoretical predictions. The alignment and calibration of the phase-shift condenser at 30 Mc is considered in detail.

PROBLEM STATUS

This is a final report on one phase of the problem; work still continues.

AUTHORIZATION

NRL Problem R12-01D
NO 284-609

AN I-F SIGNAL SIMULATOR FOR MONOPULSE RADARS

INTRODUCTION

Since in the development of improved i-f amplifiers for use in the TAB radar system, phase stability is an important consideration, convenient and accurate methods of measuring i-f phase change and of simulating radar i-f signals were desired. Since previous experiments indicated that it was possible to operate a 360° phase-shift condenser at the i-f frequency of 30 Mc with an over-all phase linearity of ± 3.5° or better, it was decided to use such a condenser as a direct-reading phase standard. Accordingly, an i-f signal generator was designed and constructed, incorporating the 360° condenser in such a way that a change in the phase shift through an external network or amplifier could be measured by introducing a compensating change within the generator and reading the value of the required shift from the calibrated dial of the condenser. In using this system, unless a correction curve is used, the absolute accuracy of a phase reading is limited to the accuracy of the calibrated condenser, in this case ± 3.5°. Small changes in phase angle may be read to within a fraction of one degree, however, since the ± 3.5° figure given above is not a random error but a smooth deviation from a linear characteristic, therefore the maximum phase error is accumulated over approximately 45° of phase change. Thus measurement of a 5° phase change within ± 0.40° can be expected. The over-all accuracy for small angles (under 45°) may be expressed as ± 7.8 percent of the measured phase interval. Measurement of small angles is, of course, limited by the phase sensitivity of the system, but this may be made greater than ± 0.1°. If correction curves are used, phase readings have an individual accuracy of ± 1°. The residual uncertainty after corrections are applied is due, at least partially, to the inadequacy of the calibration data and should be reduced as more accurate calibrations are obtained.

The subject unit is a crystal-controlled single-frequency signal generator operating at the radar i.f. of 30 Mc, and incorporating calibrated phase and level controls that permit the i-f signals for any operating condition of the TAB radar to be simulated for test purposes. A random or periodic amplitude modulation in the audio-frequency range may be superimposed on pulse modulation to provide a wide range of signal conditions. The unit includes an internal phase detector for use in phase measurement as well as output connections which permit external mixers and null detectors to be employed.

This report includes a discussion of phase-measurement techniques by the use of a calibrated standard, the details of the design and performance of the subject unit, and descriptions of methods for the calibration of the phase-shift condenser.

PHASE-MEASUREMENT TECHNIQUE

In using a calibrated phase-shifter to measure i-f phase changes, the essential additional components are a 30-Mc signal source, a phase-sensitive mixer, an indicator for

measuring the mixer output, and phase-stable amplifiers to provide the required range of output signal level to the equipment under test. The original 30-Mc signal is fed into the 360° phase shifter and also into the mixer as a phase reference. The output of the phase shifter is amplified as required, and used to drive the i-f strip or other equipment under test.

To make a phase measurement, the output of the unit under test is connected to the second-mixer input. When the desired operating conditions have been established, a phase comparison between the two mixer inputs is made by adjusting the 360° condenser until a mixer null is obtained. This may occur when the two signals are in phase, 180° out of phase, or 90° out of phase, depending on the type of mixer and on the indicator circuit used. If the mixer requires an amplitude balance for a null indication, the level of the reference signal must be adjusted to satisfy this condition. The operating conditions of the unit under test are then changed and a new balance obtained, the phase being corrected as necessary by adjustment of the 360° condenser. The phase shift which has occurred is then the difference between the initial and final dial readings of the condenser. If the value of absolute phase shift through an i-f strip or other component is required, a dummy network having the same input and output impedances as the unit to be tested may be constructed, and the initial balance made with this network substituted for the unit. If the input and output impedances are the same, so that the dummy network may be left in the circuit without causing a mismatch when the unit is inserted for the second balance, the phase characteristics of the dummy need not be known and the absolute phase shift through the circuit in question will be given by $\phi = N \times 360^\circ + (\theta_1 - \theta_2)$. In this equation, N may be 0 or any integer, θ_1 is the initial phase-shift condenser reading, and θ_2 is the second reading. If the impedances involved are resistances, a mismatch may occur without introducing a phase error, but for any other condition the effects of the mismatch must be allowed for, or the dummy removed when the unit under test is inserted in the circuit. In the latter case, the value of θ_1 must be corrected by the amount of the phase shift which occurred in the dummy network.

GENERAL DESCRIPTION OF THE UNIT

The purpose of the development work undertaken was to assemble in convenient form, in a single piece of test equipment, all the components required for i-f phase measurements by the technique outlined above; and in addition to provide for pulse and c-w modulation of the 30-Mc outputs so that simulated i-f signals could be obtained. A block diagram of the unit is given in Figure 1. A stable 30-Mc signal source is obtained by doubling from a 15-Mc crystal-controlled oscillator. The oscillator signal is fed into two separate channels, one containing the 360° phase-shift condenser, and the other providing a reference signal for phase comparison. Both channels terminate in piston attenuators of the coplanar mutual-inductance type, calibrated from 0 to -100 db. In this way, two low-impedance outputs differing in phase according to the dial setting of the 360° condenser are provided. The phase shift through the attenuators is constant within less than 0.2° over the entire range of attenuation, 0.1° of this change occurring between 0 and 2 db. Thus the levels of the two outputs may be varied widely without introducing any appreciable error in the phase measurements being made.

The reference channel contains two amplifier stages, the first variable gain, and the second constant gain with provision made for pulse modulation of the output. The course and fine gain-controls of the variable stage allow a smoother adjustment of output level than is possible with the piston attenuators, which are simple sliding-tube designs and somewhat difficult to set precisely. Easy adjustment of level is important since it was found necessary to use a phase detector which required an amplitude balance to secure a

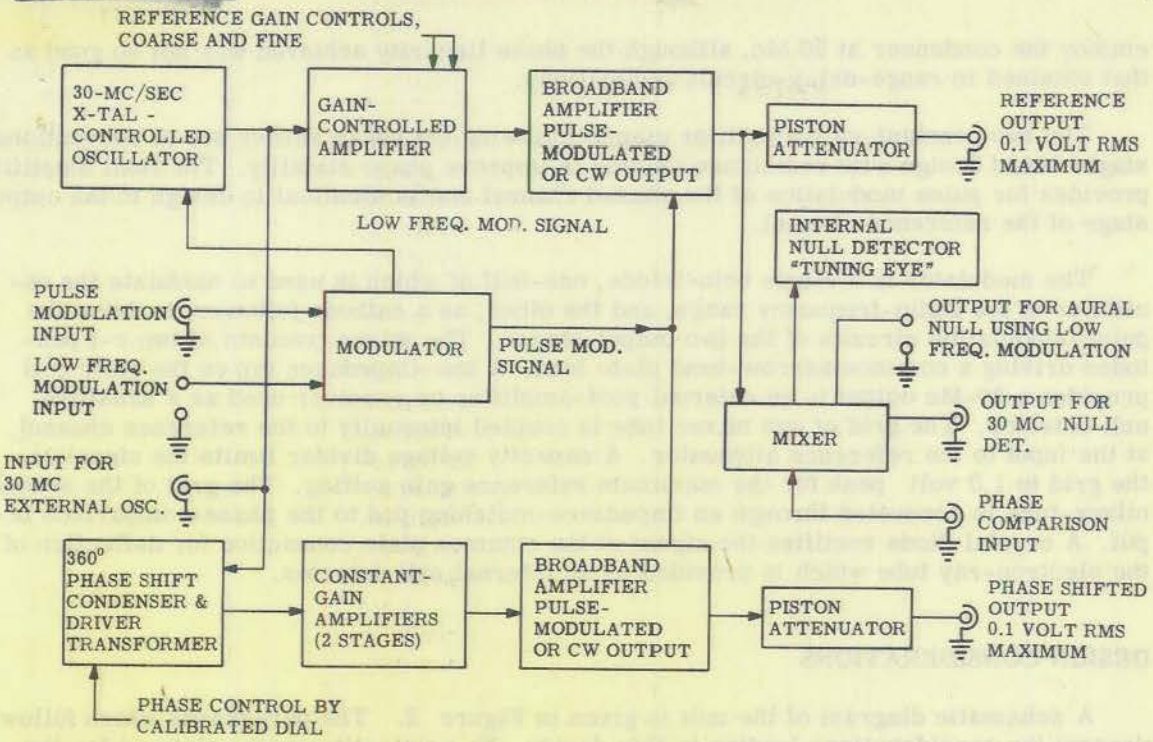

Figure 1 - Block diagram of TAB i-f signal simulator

null indication. A second reason for providing a gain adjustment other than the output attenuator lies in the high initial attenuation of this device, nearly 30 db. By connecting the reference input to the internal mixer ahead of the reference attenuator, any signal within the linear operating range of the mixer tubes may be obtained, and a wider range of phase comparison input levels may be handled. The use of the coarse gain-control requires some caution since as much as 30° of phase shift may be introduced over the full 38 db range of adjustment. The fine gain control, however, provides approximately 7 db of variation and introduces a negligible phase error for any coarse setting less than 20 db below maximum signal. Thus the fine control provides a convenient vernier even when the principal level adjustment must be made with the piston attenuator to avoid phase error.

The second reference-amplifier may be pulse-modulated by a triangular pulse as short as 0.4 microsecond or by a rectangular pulse as long as 50 microseconds without significant distortion. The low-frequency response of the circuits could be extended without difficulty if this were desired. A limiting diode is provided to prevent overdriving of the amplifier by large modulating signals. The shape of the pulse cannot, of course, be preserved when limiting occurs, but if linear operation is not required the rise and fall times of a rectangular pulse can be considerably improved by increasing the modulating signal beyond the limiting amplitude. The pulse circuits are damped so that ringing does not occur for any input rise time. Some degradation will result, however, if the input pulse has a rise time appreciably shorter than 0.25 microsecond.

The 360° phase-shift condenser is of the type used in a number of radar range circuits at lower frequencies. By lowering the impedances of the phase-splitting bridge to 56 ohms and driving the bridge with a balanced r-f transformer, it was found possible to

employ the condenser at 30 Mc, although the phase linearity achieved was not so good as that obtained in range-delay-circuit applications.

The two constant-gain amplifier stages following the phase shifter are of conventional single-tuned design with resistance loading to improve phase stability. The final amplifier provides for pulse modulation of the phased channel and is identical in design to the output stage of the reference channel.

The modulator is a single twin-triode, one-half of which is used to modulate the oscillator in the audio-frequency range, and the other, as a cathode follower, to drive the pulse-modulation circuits of the two output-stages. The mixer consists of two r-f pentodes driving a common narrow-band plate load. A low-impedance tap on the plate coil provides a 30-Mc output to an external post-amplifier or receiver used as a sensitive null detector. The grid of one mixer tube is coupled internally to the reference channel at the input to the reference attenuator. A capacity voltage divider limits the signal at the grid to 1.0 volt peak for the maximum reference gain setting. The grid of the second mixer-tube is connected through an impedance-matching pad to the phase-comparison input. A crystal diode rectifies the signal at the common plate connection for deflection of the electron-ray tube which is provided as an internal null detector.

DESIGN CONSIDERATIONS

A schematic diagram of the unit is given in Figure 2. The paragraphs which follow present the considerations leading to this design. No originality can be claimed for the mathematical analyses which are developed; they represent specific applications of well-recognized theory. Detailed derivations of the less-familiar expressions are given in the Appendices I and II.

Internal Oscillator Design

Since frequency instability of the source oscillator would cause shifts of the phase zero or reference setting as well as changes in the absolute value of the phase shift through the networks or amplifiers under consideration, crystal control of the 30-Mc internal oscillator was considered desirable. An electron-coupled doubler was used to permit a standard 15-Mc crystal to be employed and a 6AU6 tube was found satisfactory. In such a circuit, the high-frequency tank, 30 Mc in this case, is not a part of the oscillator feedback loop, and no limitations on impedance or Q exist so far as good oscillator performance is concerned. The tank circuit may therefore be designed to provide the best characteristics for the unit as a whole.

Since the unit functions as a signal generator, stray fields should be kept as weak as possible; hence the highest existing r-f potential should not be appreciably greater than that actually required in the circuit. The highest r-f voltage used exists at the primary of the driver transformer for the 360° phase-shifter and is approximately 8.0 volts rms. This value was chosen as a reasonable compromise between an excessively strong r-f field at the transformer and an inconveniently high gain amplifier following the phase shifter. Oscillator signal is also required at the input to the reference-channel amplifier, about 0.7 volt rms being needed here.

Thus, because a high r-f tank voltage was not desired, and high Q was an advantage in obtaining good 30-Mc waveform, it was decided to use a low-reactance tank having a resonant impedance just high enough to produce the required 8.0-volt driving signal,

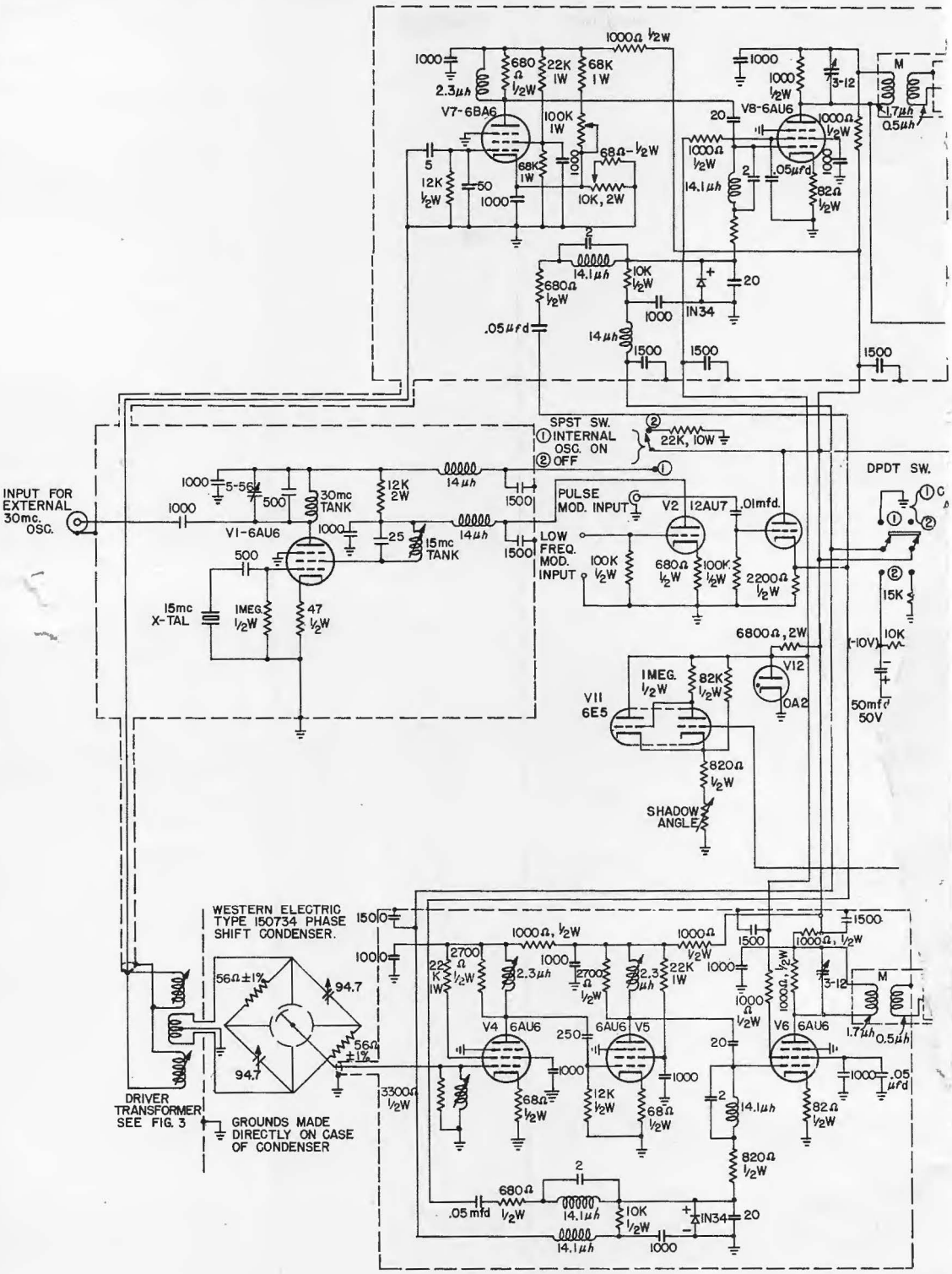

Figure 2 - Circuit diagram

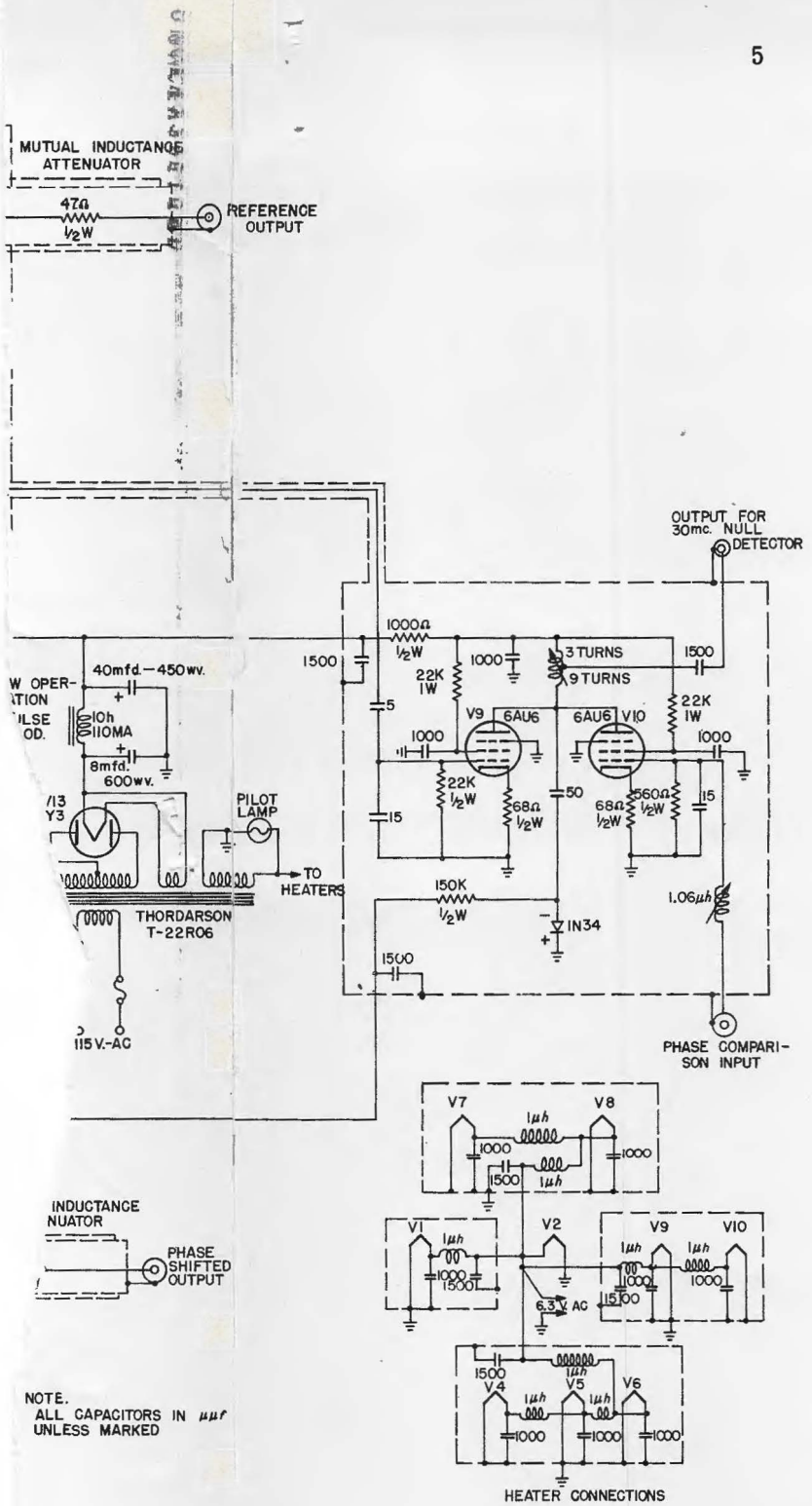
MUTUAL INDUCTANCE ATTENUATOR
47Ω
½W
REFERENCE OUTPUT
OUTPUT FOR 30mc. NULL DETECTOR
1000Ω ½W
1500
1000
3 TURNS
9 TURNS
1500
22K 1W
22K 1W
V9 6AU6
6AU6 V10
1000
1000
40mfd.—450wv.
10h 110MA
8mfd. 600wv.
22K ½W
68Ω ½W
50
68Ω ½W
560Ω ½W
15
15
PILOT LAMP
TO HEATERS
150K ½W
IN34
1.06μh
THORDARSON T-22R06
115 V.-AC
1500
PHASE COMPARISON INPUT
V7
V8
1μh
1000
1000
1500
1μh
INDUCTANCE NUATOR
PHASE SHIFTED OUTPUT
V1
V2
V9
V10
1μh
1000
1500Ω
6.3V AC
1500
V4
V5
V6
1000
1000
1000
HEATER CONNECTIONS
NOTE.
ALL CAPACITORS IN μμf
UNLESS MARKED

rather than to obtain the output by tapping down on a high-reactance tank or using coupling loops. This design also simplifies the construction of the tank coil which becomes an inductance without taps or secondary windings. The 0.7-volt input signal for the reference channel is obtained by means of a capacity divider, in which the input capacity of the tube is shunted by an additional 50 $\mu\mu$f condenser. This added capacity makes the voltage-division ratio more nearly independent of input-capacitance variations and permits the use of a lower value of grid resistance for better d-c stability, while still satisfying the phase-stability requirement that the input impedance have only a small resistive component. At the same time, the capacity variation reflected back to the oscillator tank by tube input-capacitance changes remains nearly the same since it is principally a function of voltage-division ratio, with absolute capacity a second-order effect.

Low-frequency modulation of the oscillator output from d-c to above 10 kc is accomplished by direct-coupling the screen of the 6AU6 tube, which acts as the anode of the crystal oscillator, to the plate of a dc-coupled triode modulator tube. This circuit allows up to 30% sine-wave modulation with distortion just noticeable in an oscilloscope presentation. Modulation up to 65% is possible with increased distortion of the envelope. The detected output at constant-modulation input level is 3 db down at 10 kc, and 6 db down at 20 kc. The maximum percentage of modulation is fixed by the signal-handling ability of the 12AU7 modulator, although 100% could not be obtained without a negative supply with any modulator tube. The nonlinearity of the modulation is due first to the curvature of the modulator characteristics and of the screen-voltage vs the transconductance characteristic of the oscillator-doubler; and second, to the inherent distortion caused by varying oscillator anode voltage and the transconductance between grid and tube plate simultaneously. For any frequency at which the Q of the crystal permits it to follow the modulation, the resultant variation in grid swing will add to the effect of variation of the transconductance relating the grid and the 30-Mc plate tank. Better characteristics might have been obtained by suppressor modulation of a tube designed for this service, but a negative supply would be needed to permit direct coupling and the additional complication was not thought to be justified. There is a possibility of slight frequency modulation of the crystal oscillator with the system used, but the effect should not be objectionable for broadband i-f work and it is planned to make all precise phase measurements on the basis of c-w cancellation.

Circuit of the 360° Phase-Shift Condenser

The circuit used to develop the four-phase input to the 360° condenser is basically the same as the familiar transformer and r-c bridge arrangement employed at lower frequencies in radar range-delay circuits. When this driving technique is used, the capacitances to ground from the undriven corners of the bridge and the capacitances shunting the resistive arms cause phase and amplitude errors in the bridge output voltages that cannot be entirely eliminated by any adjustment of driving voltages or of component values. To make these errors small, the impedance of the bridge must be made low compared to the stray reactances. As a reasonable compromise, 56-ohm bridge components were chosen at 30 Mc.

In order to obtain the balanced input to drive the bridge, it was found necessary to employ a physically symmetrical r-f transformer. The mechanical assembly of this transformer and the phase-shift condenser is shown in Figure 3. The secondary is made a bifilar winding to insure that each half will have as nearly as possible the same coupling to the primary, and the primary is split to provide a more nearly uniform field at the secondary location. The coupling between primary and secondary is made relatively loose to further improve the balance, and tuning slugs are provided for final adjustment. The series inductances labeled L_4 and L_5 in the figure are required to permit exact matching

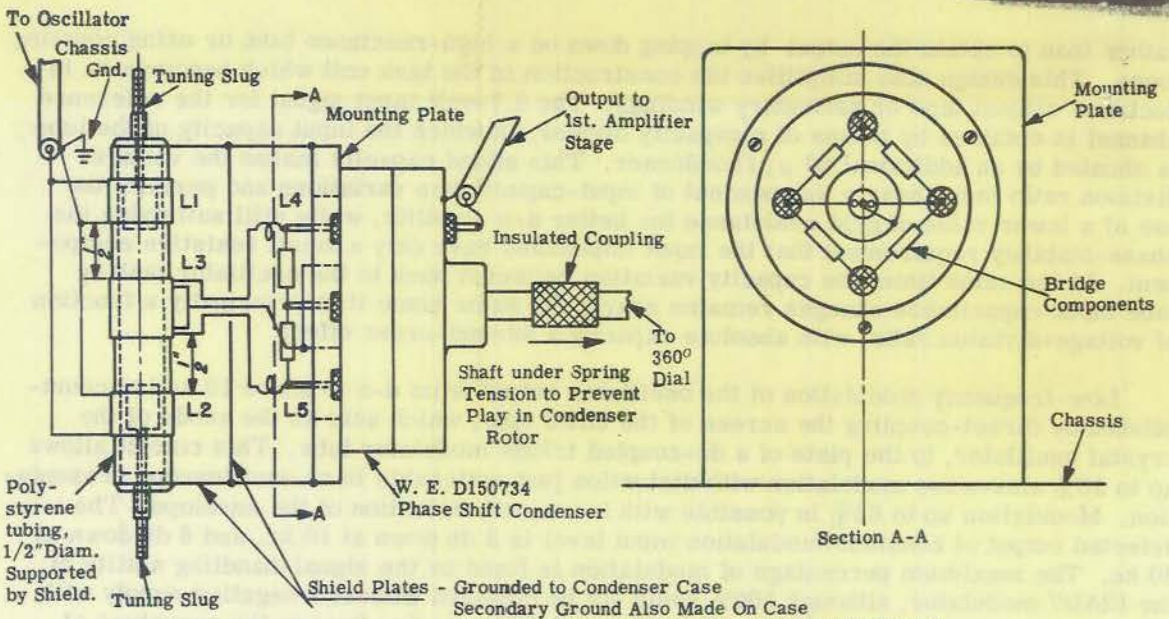

Coils:
L1 – L2 - Split Primary, 7 Turns Each Coil #18 Enameled Wire, Close Wound.
L3 - Bifilar Balanced Secondary, 4 Double Turns #18, Close Wound.
L4 – L5 - Balancing Inductors, One Or Two Turns Approximately 1/8" diameter - May Be Slug Adjustable Or "Hairpin" Type If Desired.

Figure 3 - Phase-shift condenser details

of the driving impedances for the two halves of the secondary winding. Since the secondary impedance is comparable to that of the bridge, unbalances of small percent will cause the voltages-to-ground at the driven corners of the bridge to differ, even though the voltages induced in the two sections of the secondary are exactly the same.

A shield was placed between the transformer and the bridge components, which were mounted directly on the condenser input terminals. Matched carbon resistors and silvered-mica condensers were used as bridge components. The input and output ground returns were made directly to the condenser case, and the case, in turn, was grounded to the chassis through the mounting plate. An insulated shaft coupling was used to prevent any disturbance due to r-f currents in the drive shaft. It was also found desirable to keep the shaft under light axial tension since the bearings permitted enough axial shift of the dielectric rotor to change the output phase by 1.2°. This effect was principally a detuning of the first-amplifier grid circuit caused by variation of the output capacity of the condenser. The phase linearity was equally good for any axial position of the rotor permitted by the bearings, so long as the location was not allowed to change.

The factors affecting the phase linearity which can be obtained with this condenser and circuit are discussed in detail in the section on phase calibration.

Phase-Stable Amplifier Design

In the design of the amplifier stages of the simulator the problem is one of providing a given amount of gain while contributing as little phase instability as possible. With the exception of the two pulse-modulated final stages, these amplifiers are required to

accommodate a maximum bandwidth of only 20 kc to allow audio modulation up to 10 kc. Thus, since broadband circuits are not needed, it would be possible to realize a gain of 20 or higher in one stage.

When phase stability is investigated, however, the use of two low-gain stages to obtain the required gain is found to be desirable. This may be demonstrated by consideration of the sources of phase instability in such amplifiers. At a frequency of 30 Mc transit-time effects are still small in miniature tubes and may be neglected. Thus, aside from variable differences in phase between the input and grid-cathode signals, which are found to be relatively small, changes in the phase shift through an amplifier may be regarded as due to the detuning of one or more of the coupling networks involved.

Under these conditions the phase instability of an amplifier composed of N identical stages will be N times as great as the phase instability of one stage, assuming every stage to operate under the same conditions. In addition, the instability of a single stage will increase in proportion to the size of the interstage loading resistor. Since stage gain is also directly proportional to the interstage load, we may write for an amplifier of N stages:

$$G \sim (R_L)^N,$$

and

$$\text{Phase instability} \sim N \times R_L$$

but

$$R_L \sim G^{1/N}$$

so that

$$\text{Phase instability} \sim N \times G^{1/N} \qquad (1)$$

If $G = 20$, $N = 1$

$$N \times G^{1/N} = 1 \times 20 = 20$$

If $G = 20$, $N = 2$

$$N \times G^{1/N} = 2 \times 4.47 = 8.94,$$

and an improvement of more than 2:1 is realized through the use of two stages rather than one.

For three stages:

$$N \times G^{1/N} = 3 \times 2.72 = 8.16,$$

which is only a slight improvement over two stages. Thus, two stages should probably be used to obtain a gain of 20, where the maximum phase stability is required. In many i-f amplifiers, this number of stages will be exceeded because of bandwidth requirements. In the subject unit, stage gains of 10 or lower are employed. By dividing a gain of 10 between two stages, an improvement in stability of 1.58:1 could be obtained, but stability requirements were not found to justify this complication.

To determine the best circuitry for the individual amplifier stages, the sources of instability must be considered in greater detail. Since gain-bandwidth requirements are not a limiting factor, a single-inductor interstage is the obvious choice, and all computations of stability are based on the use of this type of coupling network.

Detuning of the interstage may occur because of drifts in the values of lumped components, due primarily to temperature changes; or because of changes in the input or output admittances of the tubes involved. Changes in output admittance have been found to be small and may be considered second-order effects. The input admittance, however, includes one component dependent on stage gain and grid-plate coupling and a second component dependent on cathode-to-ground impedance, grid-cathode coupling, and the transconductance of the tube. The dependence of these electronic components of the admittance on tube transconductance causes detuning of the input circuit whenever tube electrode voltages vary. Changes in grid-cathode bias also cause variation in input capacity because of redistribution of the space charge between grid and cathode.

The input-admittance effects described, all cause phase errors because of an input-circuit detuning which changes the phase angle between the grid signal of the stage in question and the plate current of the preceding stage. In addition, if an appreciable reactance exists between the cathode and ground, the grid-cathode voltage will differ in phase from the grid-to-ground signal by an amount which depends on the magnitude of the cathode swing, and thus upon transconductance. This is a separate source of error from the effect of cathode feedback on the input admittance.

In evaluating the contribution of these effects to phase error, the following assumptions were made:

(1) That all random change in the feedback components of electronic input admittance were due to simultaneous variations in the transconductance of all the involved stages, such as would be caused by supply-voltage changes.

(2) That where variations in effective grid-cathode bias were due to variation of supply voltage only, they could be regarded as second-order effects and the components of input capacity dependent on space charge could be considered fixed.

(3) That the interaction between the various effects noted could be neglected, and each source of phase error evaluated separately.

The dependence of the input admittance on gain and on plate-grid coupling is usually called the Miller effect and is the result of feedback from plate to grid through the admittance of tube and wiring capacities. The value of the admittance due to this feedback may be evaluated as follows:

From feedback-amplifier equations, it can be shown that plate-grid coupling results in a grid-to-ground admittance which has a value

$$Y_{go} = Y_{gp} (1 \mp G) \qquad (2)$$

where Y_{gp} is the grid-plate admittance and G is the complex gain of the stage when the feedback due to Y_{gp} exists. For small values of feedback, such as exist in the pentodes being considered, G is substantially equal to the computed stage gain without feedback,

or simply $g_m Z_L$. When $Z_L = R_L$, G has no imaginary component and the reflected admittance has the same phase angle as Y_{gp} and a value $(1 \pm G)$ times as great. In a grounded-cathode amplifier the positive sign applies to G and the multiplying factor is always greater than unity.

In the 6AU6 and 6BA6 miniature pentodes used in the subject unit C_{gp} is .0035 $\mu\mu$f, C_{gk} is 5.5 $\mu\mu$f, and C_{pk} is 5.0 $\mu\mu$f. The maximum transconductance obtainable is approximately 0.005 mhos. If the effective feedback admittance were only the tube grid-plate capacity the Miller effect would be very small, but experiments indicate the 30-Mc output voltage due to grid-plate coupling when plate current is cut off is approximately 50 db below the output for a g_m of 0.005 mhos. This leads to a value of grid-plate impedance of 6.6×10^4 ohms. The phase angle of the leakage output indicates that the impedance is a capacitative reactance, and the effective coupling capacity is thus 0.08 $\mu\mu$f. The value of Y_{gp} in the equation $Y_{go} = Y_{gp}(1 + G)$ then becomes $+ j\, 1.52 \times 10^{-5}$ mhos.

The effect of cathode feedback on the input admittance is a modification of the value of the grid-cathode capacity and the introduction of a conductive term dependent on transconductance where the cathode-to-ground impedance has a reactive component. This may be expressed analytically as

$$Y_{go} = \frac{(\omega^2 C_{gk}{}^2 R_{ko} + \omega g_m C_{gk} X_{ko}) + j\omega C_{gk} (1 + g_m R_{ko} - \omega C_{gk} X_{ko})}{(1 + g_m R_{ko} - \omega C_{gk} X_{ko})^2 + (\omega C_{gk} R_{ko} + g_m X_{ko})^2} \qquad (3)$$

(See Appendix I, Eq. 22)

Sample computations using the circuit capacitances assumed above indicate that the reactive component of the admittance in the case of a by-passed or grounded cathode has a negligible dependence on transconductance for any value of incidental cathode-circuit inductance likely to be encountered. Input conductance variation with transconductance may likewise be considered a second-order effect insofar as phase stability is concerned. For the case of an unbypassed cathode resistor the susceptance term of equation (3) may be simplified with a very small error to the form

$$A_{go} = + j\omega \left(\frac{C_{gk}}{1 + g_m R_{ko}} \right) \qquad (4)$$

The second cathode-feedback effect is the phase difference which exists between the grid-to-ground signal and the grid-cathode voltage whenever the cathode impedance has a reactive component. This phase angle is expressed by

$$\theta = \tan^{-1} \left(\frac{-g_m X_{ko}}{1 + g_m R_{ko}} \right) \qquad (5)$$

where a positive angle indicates that the grid-cathode voltage leads the grid-to-ground voltage.

In comparing the influence of the effects discussed above on phase stability, the derivatives of phase angle with respect to transconductance are the most significant quantities. Letting ϕ be the angle by which the voltage developed across an interstage network leads the plate current of the preceding stage, we have

$$\frac{d\phi \text{ Miller}}{dg_m} = \frac{-\omega C_{gp} R_I R_L}{(1 + g_m R_{ko})^2} \tag{6}$$

where R_I is the load resistance of the interstage and R_L the plate load of the stage involved.

For the effect of cathode feedback on input admittance,

$$\frac{d\phi}{dg_m} = \frac{+\omega C_{gk} R_{ko} R_I}{(1 + g_m R_{ko})^2} \tag{7}$$

For the phase angle between input and grid-cathode signals,

$$\frac{d\theta}{dg_m} = \frac{-\omega L_{ko}}{(1 + g_m R_{ko})^2} \quad \text{(very nearly)} \tag{8}$$

These equations are derived in Appendix I and Appendix II, Eqs. (45), (37), and (39).

Substitution of numerical values in the expressions for the derivatives listed above show that the effect of grid-ground vs. grid-cathode phase angle is six times as small as either of the interstage detuning effects for a unity gain stage and proportionately less significant for greater gains. (See Appendix I, and Appendix II)

Considering the two interstage detuning effects together, it is clear that since the expressions for cathode and plate feedback have opposite algebraic signs, one source of detuning may be made to compensate for the other.

Setting equation (6) equal to equation (7) we have

$$\frac{\omega C_{gp} R_I R_L}{(1 + g_m R_{ko})^2} = \frac{\omega C_{gk} R_{ko} R_I}{(1 + g_m R_{ko})^2}$$

and

$$C_{gp} R_L = C_{gk} R_{ko},$$

or

$$\frac{C_{gk}}{C_{gp}} = \frac{R_L}{R_{ko}} \tag{9}$$

for exact compensation.

[redacted]

Substituting $C_{gk} = 5.5\ \mu\mu f$ and $C_{gp} = 0.08\ \mu\mu f$, we have

$$\frac{R_L}{R_{ko}} = \frac{5.5}{0.08} = 68.8\ \Omega, \qquad R_L = 68.8\ R_{ko}$$

To obtain a given gain we must satisfy the equation

$$G = \frac{g_m R_L}{(1 + g_m R_{ko})} \tag{10}$$

Since a stage gain of 10 is about the figure required for the three-tube phased-channel amplifier in the subject unit, this value is substituted below. Letting $g_m = .005$ mhos and substituting for R_L we have

$$10 = \frac{.005 \times 68.8\ R_{ko}}{1 + .005\ R_{ko}}$$

$$10 + .05\ R_{ko} = .344\ R_{ko}$$

$$0.294\ R_{ko} = 10$$

$$R_{ko} = 34.0\ \Omega$$

Then, by equation (9),

$$R_L = 68.8 \times R_{ko} = 2340\ \Omega$$

These considerations would apply to the two constant-gain stages of the phased channel. In the final pulse-modulated stages of both channels the plate-loading resistor is chosen as 1000 Ω because of bandwidth considerations. Here a 14.5 Ω cathode resistor would be needed for flat compensation.

The actual design of the amplifiers represents a compromise between the constants indicated by the theoretical considerations given and other factors of simplicity and gain stability. It was felt that more degeneration than the indicated 34 ohms was desirable from the standpoint of gain stability with tube replacement and aging. Direct-current stability could be increased while satisfying the r-f compensation requirements through the bypassing of a part of a larger cathode resistor. However, this complication was not considered justified since the effect of space-charge variations on input capacitance was neglected in the theoretical analysis of the stability problem. Experimental work done in this Sub-Section indicates that the space-charge effect is much less significant than the uncompensated Miller effect where grid-bias AGC is not attempted, but the quantitative data available is not sufficiently exact to indicate a rigorous design formula based on feedback effects alone.

An unbypassed 68 Ω cathode resistor was finally employed in each of the constant-gain stages of the phased-channel amplifier. This resulted in a 30% reduction in phase

instability due to feedback over the grounded cathode case. In the output stages of both channels 82 Ω bias resistors were found desirable to obtain maximum output without excessive waveform distortion. Bypassing of a part of this resistance was attempted but was found to distort the modulation envelope for pulsed operation because the time constant of the bypassed section was appreciable compared to the pulse rise-times which the circuit was required to handle. This caused heavy initial damping of the preceding interstage circuit followed by a recovery transient which was considered objectionable. An unbypassed 82 Ω resistor was therefore used even though it represented an over-compensation of the Miller effect in that stage.

In the gain-controlled stage of the reference channel stability of the input admittance is a less important consideration. The untuned grid circuit is shunted by an additional 50 μμf of capacity and is connected to the oscillator through a capacity divider which simulates a constant-current generator. Thus, variations of tube input capacitance have only a second-order effect on the phase of the grid voltage, and a bypassed cathode may be used without noticeably decreasing the phase stability of the unit. This permits cathode-voltage bias control which has the advantage of greater direct-current stability owing to development of a larger part of the control bias by tube current.

An unbypassed cathode resistor could be added for r-f degeneration by the resulting decrease in gain is undesirable, since it effectively reduces the control range which can be utilized. The lower gain limit is set by the level at which the output due to grid-plate capacitance and other leakage components becomes comparable to that due to plate current, and large shifts in output phase angle occur. Thus, any reduction in the maximum gain (with a given plate load) means less range of gain adjustment for the same phase error.

To increase stability and reduce variation of transconductance with plate-supply changes, all tube screens were supplied through dropping resistors from a 250-volt source. A VR tube was used to regulate the screen supply to the two output stages to maintain the same gain for c-w operation and for pulse modulation where the d-c screen current was very small.

Over-all phase stability tests of the amplifiers discussed above showed the long-time and short-time instability contributed errors smaller than the uncertainties of mixing and detecting in phase measurement. Thus, since little or no improvement in performance could be made by improving amplifier characteristics alone, no further experimental work was attempted.

Output Attenuator Design

The output-level controls of the subject unit are required to provide adjustment of signal over at least a 60-db range while introducing the least possible phase variation. Some experimental work was done with switch attenuators using standard wafers and low resistance "L" sections, but objectionable phase shifts occurred at attenuations slightly greater than 40 db even though shielding of high-level sections and careful placement of parts were employed. The experimental results indicated that high attenuations could be obtained only by placing each attenuator section and switch in a separate, shielded compartment. Under these conditions, an attenuator of the mutual-inductance type was chosen as a better solution of the problem.

Coplanar coupling was employed, since mechanical misalignment has less effect on the attenuation characteristic than in the case of coaxial coils. Also, in the coplanar case the signals due to capacity coupling and undesired modes of inductive coupling fall off more rapidly with coil spacing than does the desired signal. This may not be true when other

modes of coupling are used. The disadvantage of the mutual-inductance attenuator is the high initial attenuation, nearly 30 db in the units employed. In this respect, coaxial coupling is more advantageous than coplanar, since the two coils may be made concentric at the minimum attenuation position, giving a larger coefficient of coupling than can be obtained with coplanar coils. However, if use of the maximum possible coupling were attempted, greater nonlinearity of attenuation near the maximum coupling position would be expected, accompanied by larger phase errors. The coplanar attenuators caused almost negligible phase shifts, and had good uniformity of calibration.

PERFORMANCE DATA

Linearity of Calibrated Phase-Shift Condenser

A polar plot of the final calibration data obtained for the 360° phase-shift condenser will be presented later in Figure 10. The width of the shaded band indicates the dispersion of the calibration data at a given dial reading when all errors are referred to a starting point at 0° dial reading. These data indicate that the phase shift established by any two successive dial readings has a maximum error of ±7°, or of ±7.8% of the measured interval if the latter figure is smaller. When the calibration data are used, the error may be reduced to approximately ±2° or ±2.5%, subject to the limit of ±0.1° imposed by phase-measurement sensitivity. It is not known at present exactly how much of the dispersion in the calibration data is due to instability of the phase-shift condenser circuits and how much to errors in the data. However, single settings of the phase-shift condenser have been re-established from day to day within less than ±0.5°. This indicates that as much as 50% of the residual uncertainty of ±1° may be due to the calibration procedure. Further experimental work is planned to clarify this point. The calibration methods employed will be discussed in detail in a later section of this report.

Attenuator Calibration

Measurements of output voltage versus mutual-inductance attenuator setting indicate that the characteristic is slightly nonlinear at settings close to 0 db on the scale. The first 6 db of the scale actually represents approximately 6.9 db of attenuation, which is accumulated as follows:

0	- 2 db on scale	-	2.4 db attenuation
2	- 4 db on scale	-	2.3 db attenuation
4	- 6 db on scale	-	2.2 db attenuation
Over	6 db on scale	-	As calibrated

Since the output meter used was reliable only within ±3%, the attenuations computed have a possible error of ±0.25 db. Within these limits of accuracy the attenuation increased according to the scale calibration beyond the 6-db point.

The numbers given below represent the approximate output obtained from either channel with the piston attenuators set at 0 db. The attenuators were constructed with a 47 Ω resistor in series with the output coil to minimize resonance effects, but the phase angle of the impedance appearing at the output connector was still substantially inductive and there was considerable variation of output voltage with length for unterminated cables only a small fraction of a wavelength long.

Cable	Termination	Output
1. 39″ of RG59-U	68 Ω	30 mv
2. 39″ of RG59-U	None	60 mv
3. 6″ of RG58-U	None	110 mv
4. Open circuit at attenuator output		50 mv

The phase of the output voltage was found to shift 0.1° leading as the attenuator setting was varied from 0 to 2 db. For any further increase of attenuation beyond 2 db, the additional phase shift was less than 0.1°. These figures were obtained by establishing a phase and amplitude balance in a sensitive, external, null detector with an initial setting of 0 db on one attenuator and at least 10 db greater attenuation on the other. The attenuator settings were then increased together in 2-db steps and the phase corrections required to re-establish a null condition were noted at each step. A second set of data, taken with a 10-db initial setting on both attenuators, indicated that there was no detectable phase error due to change in mixing level. Thus, any phase corrections required represented the difference in the incremental phase shifts through the two attenuators for the given attenuation step.

Since in the coplanar attenuator the components of total coupling due to capacity and coil misalignment fall off faster with attenuation than the desired coplanar component, it is safe to assume that the phase error due to variation of these stray components will be much smaller for the 10 - 12 db step than for the 0 - 2 db step. Thus, the differential phase shift in this case may be assigned entirely to the 0 - 2 db step with only a small percentage of error. Theoretically, a second measurement would allow the 10 - 12 db phase error to be closely approximated and the original data further corrected. Since, however, the 0.1° figure obtained for the 0 - 2 db change represented nearly the smallest phase correction which could be detected, further measurements were not attempted.

Phase Measurement Errors Due to Variation of Mixing Level

In a phase-and-amplitude null detector such as that used in this unit, the normal requirement for a null indication is 180° phase opposition of the two input signals, accompanied by an amplitude match. Any stray signal coupled into the detector will, however, cause a shift in the phase relationship for a null condition unless it happens to be exactly in phase with one of the input signals. For small stray components, the maximum value of this shift is given by

$$\theta = \tan^{-1} P, \tag{11}$$

where θ is the angular deviation from 180°, and P is the fraction of the existing input signals represented by the stray component. This maximum shift will occur when the stray signal is 90° out of phase with the original inputs. For other phase relationships the phase correction will be smaller and the amplitude deviation from a balanced condition, which is zero for the 90° case, will become larger. For example, when the stray components are a minimum of 40 db below the mixer input level, the maximum error which can result from a change of mixing level from one phase reading to the next is $\pm 0.57^{\circ}$. The phase correction will become greater than that indicated by $\theta = \tan^{-1} P$, as P is increased, reaching the maximum possible value of 180° when the third component is twice as large

as the original inputs and they must be shifted from 180° opposition to phase addition in order to obtain a null. The values of the phase errors due to changes in signal level were measured experimentally for a number of different arrangements of internal and external mixers and null detectors. The results of these measurements are tabulated and discussed in the following paragraphs. In some cases the shifts in phase reading are almost entirely due to the mixing error just described, but in others phase shifts occurring in the gain-controlled channel ahead of the mixer are also significant.

The smallest changes in phase setting with mixing level were observed when the attenuator outputs from each channel were mixed in a "T" connector at the input to an external 30-Mc i-f strip. The 30-Mc amplifier was followed by a receiver consisting of a converter and broadband i-f stage, the receiver output being presented on oscilloscope for observation of the null. The data obtained were:

Attenuator Setting - db	Phase Error	Precision of Reset
0	-----	
- 10	+ 0.2°	
- 20	+ 0.2°	± 0.1° or better
- 30	+ 0.3°	
- 40	+ 0.5°	
- 50	+ 1.2°	
- 60	+ 3.2°	± 0.2°
- 70	+ 9.0°	± 1.0°
- 80	+20°	± 5°
- 90	+35°	± 5°
-100	+33°	± 8°

Note: Positive phase errors indicate a change of dial reading toward increasing lag of the phased output relative to the reference.

A second set of data was taken with the 30-Mc amplifier eliminated from the setup. Aside from the decreased sensitivity, which would be expected, these data show a much larger phase-mixing error, indicating that a stray component only some 42 db below the maximum signal existed in the receiver. This could be accounted for by radiation from the 30-Mc oscillator to the receiver, since neither device was elaborately shielded. The experimental data are:

Attenuator Setting - db	Phase Error	Precision of Reset
0	---	
- 5	± 0.2°	± 0.2°
-10	- 0.6°	
-20	- 4.3°	± 0.5°
-30	-13.8°	± 1.0°
-40	-42°	± 2.0°
-50	-92°	±10°

Additional data were taken using external mixing and adjustment of level by means of the reference channel gain control. In actual practice the reference channel attenuator would always be used for coarse level adjustment when an external mixer was used. These data are, however, of interest as a measure of the phase shift of the reference output caused

by coarse gain-control adjustment. The experimental setup was that described above, using "T" mixing and an external 30-Mc amplifier, and the phase errors for attenuator control of level are reproduced below for comparison. The differences between corresponding phase errors represent the phase shifts due to gain control action since the mixing error is the same for both cases. The data are as follows:

Attenuator Setting - db (Phased Channel)		Phase Errors	
		Reference Gain Adjustment	Reference Attenuator Adjustment
Fine Gain at Mid-Scale	0	------	----
	-10	- 0.6°	+0.2°
	-20	- 0.8°	+0.2°
	-30	+ 1.7°	+0.3°
	-35	+ 4.2°	----
	-38.5 (minimum coarse gain)	+ 8.8°	+0.5° (at -40 db)
Fine Gain at Minimum	-47 (minimum coarse gain)	+28.5°	+1.2° (at -50 db)

Another phase-comparison technique is the use of internal mixing with an i-f amplifier and receiver employed as a null detector. In this setup the output of the phased-channel attenuator was connected directly to the phase-comparison input. Reference-level adjustment was necessarily made with the gain controls. It should be noted that the internal mixer is intended to handle phase-comparison signals of 0.10 to 0.7 v rms. For this range of operation the maximum phase errors would be those for reference gain adjustment tabulated in the preceding paragraph. From the 100-Mv maximum attenuator output down, however, an appreciable mixing error appears, as shown by the following data:

Attenuator Setting - db (Phased Channel)	Phase Errors	Precision of Reset
0	------	
- 5	+ 0.5°	
-10	+ 1.6°	± 0.1° or better
-15	+ 3.7°	
-20	+ 7.5°	
-25	+14.8°	
-30	+27.0°	
-31.5	+32.6°	(Minimum Ref. Gain)

The 0-db setting of the reference gain control for this data was 15.5 db below the maximum gain position which corresponded to 0 db in the preceding data. The phase errors were, however, still larger than would be accounted for by gain-control action alone. At 30 db below maximum reference output, or nearly -15 db in the data above, the figures were 3.7° and 2.4°, leaving a 1.3° shift due to incomplete isolation of the internal mixer. The increase in error from -15 db to -30 db in the earlier data was 2.4°. This

differential phase error may be used to make an indirect computation of the leakage level at the mixer. From the mixing-error formula in Eq. (11) a stray component a maximum of 33 db below the existing input signal level would account for a 1.3° shift. For phase relationships other than 90° a higher-level leakage could exist. Thus, the stray signal coupled into the internal mixer has the effect of a signal at the most unfavorable phase angle, 63 db below the maximum mixer input of approximately 0.7 volt rms.

When internal mixing is used, the experimental setup may be simplified by eliminating the i-f amplifier and using only a 30-Mc receiver and oscilloscope as a null detector.

Attenuator Setting - db (Phased Channel)	Phase Error	Precision of Reset
0	-----	
- 5	+ 0.4°	
-10	+ 1.4°	
-15	+ 4.0°	
-20	+ 8.5°	±0.2° or better
-25	+16.0°	
-30	+31.5°	
-31.5	+37.0°	

Comparison of this data with that in the preceding paragraph shows that the higher relative level of stray signals in the receiver in the absence of the 30-Mc i-f amplifier has an effect on phase errors, but this is at worst a 15% increase. This is a much smaller change than that noted earlier when the amplifier was eliminated in the case of external mixing since the level at the receiver input is increased by the gain of the internal mixer, which performs as a narrow-band pentode amplifier.

The electron-ray tube of the unit provides a convenient but relatively insensitive null indication for the internal mixer.

Attenuator Setting - db (Phased Channel)	db Below Max. Mixer Input	Phase Error	Precision of Reset
0	15	+1°	± 0.5°
- 5	20	--	± 1.0°
-10	25	--	± 5°
-20	35	--	±10°

This data is of interest chiefly as an indication of the relative precision of the phase readings. Mixing errors the same as those noted for more sensitive null detectors would be expected, but are masked by the reset error.

To employ aural null detection, a set of phones was connected to the mixer-detector output and audio modulation applied to the 30-Mc oscillator to produce a tone which would indicate relative signal level. The following data were recorded:

Attenuator Setting - db (Phased Channel)	db Below Max. Mixer Input	Precision of Reset
0	15	± 2°
-10	25	± 5°
-20	35	±15°

The accuracy of this means of null detection is seen to be somewhat poorer than that obtained using the electron-ray tube as a detector. This is partly due to harmonics of the audio modulation which exist in the mixer modulation envelope because of nonlinearity in the oscillator modulation characteristics as well as in the amplifiers. This situation is complicated by the fact that the characteristics of the two channels do not "track" exactly, and thus a relatively broad minimum rather than an absolute null is likely to be found. In general, the minimum for the fundamental will not occur at exactly the same r-f phase as do those for the higher harmonics. It is possible for the ear to recognize a given condition arbitrarily designated as the null setting, but there is some uncertainty involved. The tone obtained was also rather weak for work in the presence of any external noise. An audio amplifier would undoubtedly increase the sensitivity, but amplification at 30 Mc as discussed earlier would be preferable.

A 30-Mc postamplifier may also be used to detect a null in a modulated signal output from the internal mixer. The results obtained with this technique are tabulated as follows:

Attenuator Setting - db (Phased Channel)	db Below Max. Mixer Input	Phase Error	Precision of Reset
0	15	------	
- 5	20	- 0.4°	
-10	25	+ 0.2°	
-15	30	+ 2.7°	±0.2° or
-20	35	+ 6.9°	better
-25	40	+15.2°	
-31.5	46.5	+37.2°	±0.5°

The data obtained by this method show substantially the same phase errors as were found for the use of external 30-Mc c-w null detection and the precision of reading is equivalent to that shown for a receiver and scope combination. However, this accuracy could be obtained only by viewing the postamplifier output on a scope where some particular cancellation point could be recognized and designated as the null setting. The use of an output meter sensitive to average modulation level gave relatively broad null indications for the reasons discussed for aural null detection.

The best phase-measurement accuracy over a wide range of signal levels was obtained by mixing externally to enable level adjustment to be made entirely by means of the output attenuators, which have a negligible phase error. In using this method the stray signal at the final mixer or detector must be kept small compared to the desired signal. A 40-db difference in level will limit phase errors to ±0.6°. The limitation of external mixing is that only signals within the range of the reference channel output may be balanced. If higher-level signals, such as the output of an i-f strip, must be handled, an auxiliary attenuator must be inserted or the internal mixer used.

Internal mixing requires the adjustment of reference-channel level by means of a gain-controlled amplifier stage which introduces some phase error. This error is less than 2° for any setting within 30 db of maximum gain and less than 10° over a 38-db range, but increases rapidly for greater gain reductions, reaching 28.5° at the minimum-gain position of the controls.

The reset error obtained with either internal or external mixing depends only upon the sensitivity of the null detector used. Since the maximum precision of a phase-dial reading is 0.1 degree, a reduction of reset error much below $\pm 0.1^\circ$ has little advantage. This order of precision was easily attained for a mixing level as much as 50 db below the 100-millivolt maximum attenuator output when external null detectors were used. The use of the internal electron-ray tube as a c-w null detector gives a reset error of $\pm 1.0^\circ$ within 20 db of maximum reference signal and $\pm 10^\circ$ over a 35 db-range.

The methods discussed above all assume the use of a c-w r-f null detector. The 30-Mc signal may, however, be modulated in the audio range and the detected modulation envelope used as a null criterion. The use of earphones connected at the grid of the electron-ray tube gives somewhat poorer accuracy than the visual indication. A 30-Mc postamplifier may yield as great sensitivity as any c-w detector but the nonlinearity of the modulation envelope obtained, and the fact that the envolopes are not identical for the two channels make the null setting less precise for the same overall gain.

Stability of Phase-Dial Readings

In making warmup checks the first phase-dial reading was recorded after an initial stabilization period of two minutes. Any auxiliary test equipment used was allowed to stabilize completely before the unit was switched on. Under these conditions the following shifts in dial reading were observed.

Warmup Time - Minutes	Phase Increment	Total Accumulated Drift
2 - 5	-0.9°	-0.9°
5 - 10	-0.5°	-1.4°
10 - 15	-0.5°	-1.9°
15 - 20	-0.4°	-2.3°
20 - 30	-0.2°	-2.5°
30 - 40	-0.3°	-2.8°
40 - 60	-0.2°	-3.0°
60 - 90	-0.0°	-3.0°
90 - 130	-0.1°	-3.1°

The negative signs of the phase increments listed above indicate that decreasing dial readings were required to re-establish a null condition as warmup progressed. Thus, the phase shifts which occurred in the unit had the effect of causing the phased output to lag the reference by the angles given.

The data given below indicate the effect of rapid fluctuations in line voltage above and below the value of 115 v, at which the subject unit was allowed to stabilize. The power supply of the unit was a conventional unregulated full-wave design. The algebraic signs of the phase shifts listed below have the same significance as those in the preceeding paragraph.

Line Voltage	Deviation	Error of Phase Dial Reading
115	0	------
112	- 2.6%	-0.2°
110	- 4.3%	-0.7°
105	- 8.7%	-0.8°
95	-17.4%	-1.0°
120	+ 4.3%	+0.4°
125	+ 8.7%	+0.7°
135	+17.4%	+1.5°

The phase errors caused by variation of oscillator signal level were measured for two conditions. For the first set of readings the reference gain controls were set for maximum gain; for the second, at 20 db below the maximum. The oscillator voltage was measured with a probe connected at the primary of the phase-shift-condenser transformer. Comparison of the two sets of data indicates that the phase shift vs. signal level characteristic of the gain-controlled amplifier is a function of gain setting. However, considering the small variations of oscillator level which would be expected in normal operation, the phase errors are not serious for either condition tabulated.

Oscillator Level Volts R.M.S.	Error of Phase Dial Reading	
	Maximum Reference Gain	-20-db Reference Gain
8.1 (max)	------	-----
7.0,- 1.3 db	-0.1°	-----
6.0,- 2.6 db	-0.2°	-----
5.0,- 4.2 db	-0.2°	-----
4.0,- 6.1 db	-0.3°	-0.8°
2.0,-12.2 db	-0.5°	-1.2°
1.0,-18.2 db	-0.6°	-1.5°
0.5,-24.2 db	-0.5°	-----
0.2,-32.2 db	-0.8°	-2.1°

Variation of Output Signal Level

Due to detuning of the high-Q 30-Mc doubler tank, the outputs from the unit are reduced in level until warmup is completed. The relative levels checked during a one-hour warmup period are tabulated below:

Warmup Time - Minutes	Output Signal Level
2	-8.2 db
5	-7.1 db
10	-5.3 db
15	-3.8 db
20	-2.5 db
25	-1.6 db
30	-1.0 db
40	-0.6 db
60	0 db

Input and Output Impedances

The input and output impedances were measured at the ends of several representative connecting cables, such as might be used with the unit. These cables are listed below. The length figures indicate the amount of free cable between connectors, a type N to type BN adapter being added at the input connector of the subject unit when using BN to BN cables.

Cable	Type	Nominal Characteristic Impedance	Connectors	Length
A	RG-58-U	52 ohms	BN to BN	5-3/4"
B	RG-59-U	72 ohms	N to BN	6-1/2"
C	RG-58-U	52 ohms	BN to BN	10-1/2"
D	RG-59-U	72 ohms	BN to BN	28"
E	RG-59-U	72 ohms	BN to BN	39-1/2"
F	RG-58-U	52 ohms	N to BN	61"

The impedance measurements were made with a General Radio Type 916-A, R.F. Bridge, Serial No. 430. The bridge dial readings were corrected for a frequency of 30 Mc, to obtain the final impedance values tabulated.

The phase-comparison input impedance was measured using each of the cables listed above, and in addition another set of measurements was made to show the effect of mixer-tank detuning on the value of the input impedance. An "L" pad was used to obtain a voltage step-up to the grid of the phase-comparison mixer stage and variation of the tube input reactance with plate tuning was found to affect the impedance transfer through the pad by as much as 16% of the normal value of input impedance. This maximum deviation was obtained only by deliberate misalignment of the mixer tuned circuit to an extent which would never occur as a result of warmup drifts, aging, etc. However, this effect was responsible for the use of a low-Q, broadband "L" section having much less voltage step-up than could have been theoretically attained. Higher Q-pads were tested and found to be objectionably unstable.

Cable Used	Phase Comparison Input Impedance (ohms)	Condition
A	71.2 -j 5.7	Normal operation
B	74.0 +j 0.5	Normal operation
C	68.5 -j10.7	Normal operation
D	72.0 -j 1.1	Normal operation
E	69.7 -j 0.6	Normal operation
F	40.2 -j 1.9	Normal operation
E	69.7 -j 0.6	Normal operation
E	74.8 +j 2.3	Mixer tank detuned, - 6 db
E	83.4 +j 1.4	Mixer tank detuned, - 9 db
E	87.0 -j 8.32	Mixer tank detuned, -12 db
E	61.2 -j 7.8	Plate supply & heater voltage removed from Mixer.

The following data were obtained by measurements on the reference-channel attenuator. The phased-channel attenuator was identical in construction and should have substantially the same impedance values. No change in the output impedance with attenuation setting could be observed.

Cable Used	Attenuator Output Impedance (ohms)
A	185 -j 117.0
C	262 -j 30.5
D	170 -j 126
E	65.6 -j 97.9

The null-detector output connection is a tap on the mixer tank placed to give an impedance step-down of approximately 16:1. The impedance values listed below were measured with the tuned circuit "peaked" for normal operation.

Cable Used	Null Detector Output Impedance (ohms)
A	237 -j 161
B	338 -j 186
C	100 -j 140
D	42.6 -j 78.7
E	26.8 -j 47.6
F	11.3 -j 8.7

The external oscillator input is connected across the entire doubler tuned-circuit and the impedance is too high to measure with any accuracy on the r-f bridge used for the other impedance measurements. The impedance may be estimated from the value of tank reactance and the expected Q, or from output voltage and plate-current swing. These approximations place the impedance between 1000 and 1500 ohms. The phase angle of this impedance will be sensitive to doubler-tuning since the circuit Q is over 100, but it should remain predominately resistive during normal operation of the unit.

Pulse-Modulation Characteristics

The pulse-modulation circuit of the subject unit was designed to permit pulse modulation of the 30-Mc i-f output up to the normal c-w level. Since control-grid modulation is used, the modulating signal must be limited at approximately the c-w operating point of the tube if grid current loading is to be avoided. A diode, used for this purpose, has the effect of squaring the modulating pulse whenever it exceeds the critical level. Since the modulating cathode follower has enough dynamic range to develop a signal several times the critical level without input loading, considerable improvement in pulse edges may be obtained by taking advantage of the diode limiting-action where linear modulation is not required.

The pulse circuits are damped heavily enough to prevent overshoot, or ringing, with short input-rise-times. For input-rise-times as short as 0.25 microseconds the modulation envelope shows only a slight degradation of pulse shape. An unlimited modulating pulse having a rise-time of 0.27 μsec between 10% and 90% points produced an envelope

having an 0.34 μsec rise. For shorter input rise times there is a greater proportional increase in envelope rise time. A limited modulating pulse of 0.09 μsec rise produced 0.18 microseconds rise in the 30-Mc envelope.

The pulse-modulation envelope is not affected by gain-control or attenuator adjustments. The same circuit is employed in both channels and there is no observable difference in modulation characteristics.

The level of the c-w leakage which exists between modulating pulses depends upon the negative bias applied to the output-tube grids. A bias of -10 volts reduces the leakage level to at least 58 db below the maximum pulsed-output. A further increase in bias reduces leakage by only 1 or 2 db. A -9.5-v bias was used, but lower bias voltages may be used if slightly higher leakage levels can be tolerated. A decrease in bias makes the pulse modulation more nearly linear at low levels and this advantage must be weighed against the disadvantage of a larger c-w component in the output.

Where a -9.5-v bias is used, a 9.8-v pulse at the modulation input jack will produce a noticeable 30-Mc pulsed output. At a 22-v peak-input amplitude the diode limiter becomes effective, and at 38 v the input cathode follower begins to draw grid current.

C-W Modulation Characteristics

Sine-wave modulation up to approximately 30% may be produced with harmonic distortion barely noticeable in an oscilloscope presentation. Above 30% modulation the distortion increases considerably because of modulation-amplifier nonlinearity and other factors which have been discussed under Internal Oscillator Design. The required sinusoidal modulating signal levels for various conditions are tabulated below.

Signal at Low-Frequency Modulation Input (Volts R. M. S.)	Percentage Modulation	Remarks
1.0	12.5	Very slight distortion.
2.0	26.5	Very slight distortion.
3.0	34.0	Very slight distortion.
5.0	----	Noticeable distortion.
10.0	----	Mod. Amp. overdrives.
20.0	68.0	Max. obtainable modulation, waveform approaches a square-wave.

The frequency response of the modulator extends slightly beyond the audio spectrum The response is down 3 db at 10 kc and less than 6 db at 20 kc.

ACCURACY OF THE PHASE-SHIFT CONDENSER

Sources of Error

A detailed theoretical analysis of the Western Electric phase-shift condenser was presented in an NDRC report from the Radiation Laboratories, M. I. T., to NRL dated 12-26-44. The report is titled, M. I. T. No. 633, "Errors in the Western Electric Phase Shift Condenser," NRL File Number 024418, and is the basis for the estimates of attainable accuracy which are made. There are four major sources of error; approximations

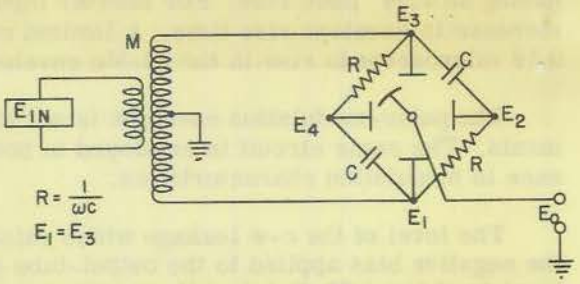

Figure 4 - Bridge driving-circuit for the phase-shift condenser

made in the mechanical design of the condenser, stray reactances in the input bridge circuit errors in driving voltages, and errors in bridge component values. These factors are discussed separately below.

To increase ease of production, the dielectric rotor of the Type D150734 condenser was machined in the form of an eccentrically mounted circular disc instead of the cardioid shape which is theoretically required. This approximation causes an output phase error which varies over a $\pm 0.7^{\circ}$ range as the rotor position changes. The varying phase error is accompanied by an output amplitude fluctuation of about $\pm 1\%$.

Various methods may be used to drive the condener, and the one chosen will determine the contributions made by the last three sources of error listed. The circuit shown in Figure (4) is best suited to r-f work and was used in the subject unit. This bridge circuit will produce matched four-phase driving voltages only if the bridge arms are pure resistances and reactances, and if the stray impedances to ground from the undriven corners of the bridge are so high as to cause negligible loading. In the condenser under consideration the stray impedances are essentially capacitative reactances. The stray capacities and their magnitudes are indicated in Figure 5. The stray capacities shunting the capacitance arms of the bridge are, of course, lumped with the added capacity to make up the correct value, and cause no errors. Capacity loading of the resistance arms, however, causes phase and amplitude errors in the voltages developed at plates (2) and (4) of the condenser, and these errors cannot be completely compensated by any adjustment of the bridge arms. Thus, to keep the effect of the shunting reactances small, the resistances of the bridge must be lowered as the operating frequency is raised. The capacities to ground at plates (2) and (4) likewise cause phase and amplitude errors which can be kept small only by making the impedance of the bridge low compared to the stray loading. It would be possible to reduce loading errors by resonating the stray capacitances with suitable inductors. Since, however, the capacitances from plates (2) and (4) to ground vary by $\pm 8\%$, depending on the position of the dielectric rotor, tuning would not be entirely effective here.

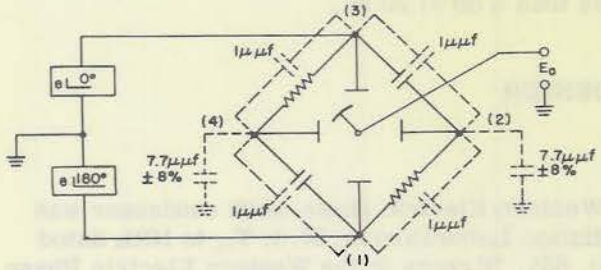

Figure 5 - Stray capacitances in the bridge driving-circuit

Deviation of the bridge driving-voltages to ground at plates (1) and (3) from matched amplitude and 180° phase opposition causes proportional phase and amplitude errors in the output voltage. There is no theoretical limit to the accuracy with which these voltages may be adjusted, but the separate phase and amplitude control required constitutes a practical problem. Also, as the frequency is raised it becomes increasingly difficult to determine the accuracy of the driving-voltage adjustment other than by actually measuring the linearity of the output phase versus rotor angle. Output amplitude flucutations are an indication of some maladjustment but may be due to errors in bridge components rather than to errors in driving voltages. Thus, when any other errors exist there will be a range of adjustment of driving voltages over which amplitude variations with rotor angle will not change appreciably, and there will be no indication as to which adjustment in this range actually gives the best output phase linearity. However, for any driving voltage adjustment within the critical range the phase errors contributed should be comparable to those which exist because of bridge loading and misadjustment. Thus, amplitude fluctuation is a good criterion for preliminary adjustment, and will be an increasingly good measure of accurate alignment as the errors due to misadjustments other than the one being corrected are made smaller.

Incorrect values of resistance or capacitance in the bridge arms will cause output phase and amplitude errors similiar to those caused by driving-voltage misadjustment. The reduction of these errors is a question of technique in the accurate measurement of initial values and in the choice of components which are stable with respect to ambient temperature and aging. At frequencies as high as 30 Mc, carbon or metallized resistors are the only convenient elements for the resistance arms of the bridge, and resistance stability is thus limited by the relatively poor characteristics of these units. The capacitance arms of the bridge can be stabilized to a high degree by using a combination of negative and positive temperature-coefficient capacitors, but too great refinement here is pointless when carbon resistors are used in the resistance arms.

Evaluation of Errors

The table given below lists the principle sources of error discussed above and the formulae which may be used to compute output phase errors for given input circuit discrepancies.

The symbol $\Delta\theta$ used in the table represents the maximum angle by which the phase of the output voltage leads the mechanical angle of the condenser rotor. The rotor angles listed in the Maximum Error column are measured from the point at which the rotor is set for maximum coupling to the input plate at E_1 in Figure (4). The algebraic signs given are the signs of the errors when $\Delta\theta$ is positive. Where the criterion of output phase is the instant at which the complex output voltage passes through zero (or some other desigated point) harmonic distortion of the driving voltages will cause phase errors. The error for second harmonic distortion of q percent is given by

$$\Delta\theta = \frac{q}{5} \times \frac{2\pi}{100} \text{ radians,}$$

if the impedance shunting the condenser output has the same value for fundamental and second harmonic. Where the phase-shift condenser is followed by a tuned amplifier having good rejection for the harmonics of the driving signal, so that the phase of the fundamental itself is the criterion for phase comparison, harmonic distortion causes no error. This is the case in the present unit.

TABLE I
Phase Error Formulae

Source of Error	Phase Deviations	Rotor Angles for Maximum Errors
Approximation in mechanical design of rotor	± 0.7 (degrees)	(-) (+) (-) $\frac{\pi}{8}, \frac{3\pi}{8}, \frac{5\pi}{8}, \cdots$
Capacitances to ground at undriven corners of bridge	$\Delta\theta = \frac{-Cg}{4C}$ (radians) Where C is the bridge capacitance, Cg the stray capacitance.	(+) (-) (+) $\frac{\pi}{4}, \frac{3\pi}{4}, \frac{5\pi}{4}, \cdots$
Reactance of resistance arms of bridge	$\Delta\theta = \frac{+Xs}{2R}$ (radians) Where Xs is the equivalent series reactance and R is the resistance of the bridge arms.	(+) (-) (+) $\frac{\pi}{4}, \frac{3\pi}{4}, \frac{5\pi}{4}, \cdots$
Phase error of the driving voltage of E_1	$\Delta\theta \leqq \begin{cases} -\frac{3}{2}\ \Delta\phi \\ +\frac{1}{2}\ \Delta\phi \end{cases}$ (radians) Where $\Delta\phi$ is the phase error of the driving signal.	$\left(+\frac{3}{2}\right) \left(-\frac{1}{2}\right) \left(+\frac{3}{2}\right)$ $0, \pi, 0, \cdots$
Difference in amplitude of driving voltages E_1 and E_3	$\Delta\theta \leqq +\frac{\Delta A}{2A}$ (radians) Where ΔA is the amount by which the signal at E_1 exceeds that at E_3 and A is the normal amplitude.	(-) (-) (+) (+) $\frac{\pi}{4}, \frac{3\pi}{4}, \frac{5\pi}{4}, \frac{7\pi}{4}, \cdots$
Error of P percent in value of the R or C arm of the bridge adjacent to E_4	$\Delta\theta = \pm\frac{3}{2} \times \frac{P}{100}$ or $\pm\frac{1}{2} \times \frac{P}{100}$ (radians) Where the upper signs apply for R errors and the lower for C errors.	$\left(-\frac{1}{2}\right) \left(+\frac{3}{2}\right) \left(-\frac{1}{2}\right)$ $\frac{\pi}{2}, \frac{3\pi}{2}, \frac{\pi}{2}, \cdots$
Error of P percent in both R or both C arms	$\Delta\theta = \frac{\pm P}{100}$ (radians) Where the upper sign applies for R errors and the lower for C errors.	(+) (+) (+) $\frac{\pi}{2}, \frac{3\pi}{2}, \frac{\pi}{2}, \cdots$

It would appear from the angles for maximum error listed in Table 1 that the errors caused by stray capacitance to ground, or by reactance of the resistance arms, might be reduced by deliberate misalignment of the bridge or driving voltages. This would be true at the maximum error points themselves, but since the various error functions do not "track," good correction would be obtained only over narrow bands of dial readings and the over-all accuracy might not be greatly improved.

Comparison of Design and Input-Circuit Errors

Since the design approximation of the phase-shift condenser results in an unavoidable error of $\pm 0.7^0$ it is desirable to calculate what degree of refinement of the input circuit is justified. An approximate figure may be obtained by treating the phase-error functions as if they were sinusoidal functions having the periods indicated by the maximum-error column in Table I. This tabulation indicates that the error function due to condenser design has a period of $\pi/2$ radians of mechanical rotation while the input-circuit error functions all have periods of π or 2π radians. Under these conditions, the most unfavorable combination of input-circuit misalignments is found to yield a maximum error approximately four times as great as one of the individual errors if all the sources involved are assumed to contribute the same phase deviation. Thus to avoid the possibility of doubling the design error, the individual input-circuit errors must be limited to approximately $0.7^0/4 = 0.18^0$.

Computation of Input-Circuit Errors

In the following calculations it is assumed that no attempt is made to neutralize the stray capacities of the condenser. It is further assumed that standard carbon resistors will be used as the resistance elements of the driving bridge; and that, since temperature control of the bridge circuits will not be employed, the bridge components will be subjected to variations in operating temperature as the ambient temperature changes. The error formulas used are taken from Table 1.

For capacitance to ground at the undriven corners of the bridge we have:

$$\Delta\theta = \frac{-Cg}{4C} = \frac{-7.7 \times 57.3}{4 \times 94.8}$$

$$\Delta\theta = -1.16^0$$

The effect of reactance of the resistance arms of the bridge is computed as follows:

Shunting Capacitance = 1.0 mmf (approx.)

$$X_C = \frac{-10^6}{188.5 \times 1.0} = 5{,}305 \text{ ohms}$$

Assuming that the resistor itself has a negligible phase angle, which is true of a 1/4 W, 56-ohm carbon unit at 30 Mc, we have

$$Z = \frac{56(-j5305)}{56 - j5305} = (56 - j0.59) \text{ ohms}$$

Thus $X_S = -0.59$ ohms and $\Delta\theta = \frac{(-0.59)}{(2 \times 56)} \times 57.3 = -0.3^\circ$

Bridge component errors depend largely on the stability of the units available. A typical carbon resistor will have a temperature coefficient of about 0.05% per degree Centigrade. Thus, for an ambient temperature ranging from 60° to 100°F, the variation will be 1% (or ±0.5%) about an average operating temperature. In contrast to this, a silvered-mica capacitor will have a coefficient of only about 0.002% per degree C, or ±0.02% over a 60°-100°F range. Resistor stability is thus the limiting factor, and temperature compensation of the condensers is not justified.

For an error in one bridge arm of +0.5%

$$\Delta\theta = + 3/2 \times 0.5/100 \times 57.3 = + 0.43^\circ$$

$$\Delta\theta = - 1/2 \times 0.5/100 \times 57.3 = - 0.14^\circ$$

For simultaneous 0.5% errors in both R or both C arms

$$\Delta\theta = \pm \frac{0.5}{100} \times 57.3 = \pm 0.29^\circ$$

For a phase error of the driving voltage we have

$$\Delta\theta = - 3/2 \ \Delta\phi, \text{ and } + 1/2 \ \Delta\phi,$$

where $\Delta\phi$ is the deviation of one driving voltage from the correct phase.

For

$$\Delta\phi = 1^\circ$$

$$\Delta\theta \leqq - 1.5^\circ, + 0.5^\circ$$

For an amplitude error of the driving voltages:

$$\Delta\theta = + \frac{\Delta A}{2A}$$

For a ± 1% difference in amplitude:

$$\Delta\theta = \pm \frac{.01}{2} \times 57.3 = \pm 0.29^\circ$$

The phase-error computations presented above show that if the errors from all sources are to be comparable, the bridge components must be matched within slightly better than 0.5% and must not deviate more than an additional 0.5% from their initial values. Further, the amplitudes of the driving voltages must be matched within 3% and must differ from a 180° phase relationship by less than 1.0°. When these requirements are satisfied, each

source of error will contribute maximum deviations of approximately ± 1.0°, and these errors will add under the least favorable conditions to give peaks about four times as great, or ± 4.0°. The design error of the condenser may add to this error to increase the peak to about ± 4.7°. If only the errors due to stray capacities and design exist, the peak deviations possible are ± 2.2°.

PHASE CALIBRATION

Possible Experimental Techniques

Since phase angle is basically a measure of a time interval, all phase measurements are fundamentally time measurements regardless of the method used. The experimental techniques which may be employed fall into three roughly defined groups according to the time base to which the unknown phase interval is referred for evaluation.

In the first group are methods employing an independent time base used to measure the phase interval by a comparison method. These methods can be applied to the case of any periodic function regardless of harmonic content. The time interval measured may then be converted to an angular quantity whenever the frequency of the function is known. These techniques may be used with considerable precision at low frequencies, where scope presentations similar to the radar "A" presentation may be used to compare intervals, but become unusable at radar i-f frequencies.

The second group includes methods in which the time base is supplied by the reference signal to which the phase interval is referred, and the basis of measurement is essentially the comparison of the unknown interval to a complete cycle of the reference. The familiar scope presentation, in which the two signals are applied to the horizontal and vertical plates respectively, is an example of this technique. The mixing of the two signals and the computation of phase from the relative output is a second example. The application of this technique to 30-Mc signals will be discussed in detail later. In both of the examples given, the phase angles are calculated on the assumption that the voltages involved are pure sine functions; any harmonics present will introduce errors which are difficult to evaluate.

The third group of techniques may be considered a refinement of the methods falling into the second group. Here one cycle at the fundamental frequency is accurately subdivided by frequency multiplication of both the involved signals. By this means, errors caused by harmonic content and limitations of detector sensitivity or scope resolution are reduced almost in proportion to the order of the harmonic employed. Where multiplication leads to frequencies too high to be conveniently handled, a common local oscillator may be used to heterodyne the original signals to a lower frequency before multiplication.*

Theoretical Basis for Mixer Method of Phase Measurement

If two sinusoidal voltages are added algebraically in a linear network, the output voltage is a function of the phase angle between the two inputs. Thus, if the constants of a network are known, the phase angle between two applied signals may be computed from measurements of relative amplitude. The material presented below discusses the form of the

---

* *This last method, when applied to the 30-Mc phase problem by another member of this sub-section, yielded results superior to any previously used technique. The phase-shift condenser calibration obtained by this method is included in this report. The method is to be described in detail in a later memo.*

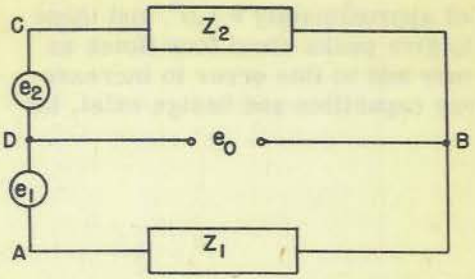

Figure 6 - Balanced mixer

output function for a simple mixer which can be realized physically at 30 Mc. The precision of phase measurement which can be obtained is calculated in terms of the deviation of voltage magnitudes and network component values from the theoretically correct conditions of balance In the following sections the experimental procedure used in calibrating the subject unit is described and the expected accuracy of calibration is computed from the experimental data.

The form of mixer used for 30-Mc phase measurement is diagramed in Figure (6).

In this figure:

$$e_{DA} = e_1 \angle 0^\circ$$

$$e_{DC} = e_2 \angle \theta^\circ$$

$$e_{DB} = e_0$$

The expressions relating the input voltage, output voltage, and phase angle are derived in Appendix III, Equations (47) to (54). In this derivation it is assumed that the impedances Z_1 and Z_2 are closely matched and that e_1 and e_2 are nearly equal in magnitude. Under these conditions it is convenient to define the following terms:

$$\frac{Z_1}{Z_1 + Z_2} = a - jb$$

$$e_1 = e$$

and

$$e_2 = e\,(1 + \Delta)$$

where $Z_1 = Z_2$, $a = 0.5$ and $b = 0$. Employing these definitions, we have

$$e_{om} = e\sqrt{1 + \Delta^2 a^2 - 4(a - a^2 - b^2 - \Delta a^2)\sin^2\frac{\theta}{2} + 2\Delta a \cos\theta + 2(1 + \Delta)\, b \sin\theta} \qquad (12)$$

where e_{om} is the magnitude of the complex output voltage e_0. Thus

$$e_0 = e_{om} \angle \gamma^\circ$$

Terms having the higher powers of b and Δ as factors have been dropped from this equation, but these omissions will cause negligible errors unless b or Δ exceeds a value of 0.1. In the experimental circuit employed, these quantities are well within this limit and equation (12) may be applied.

Where $b = \Delta = 0$, equation (12) reduces to the form

$$e_{om} = e \cos \frac{\theta}{2}, \tag{13}$$

and the computation of phase angle becomes very simple. It is, therefore, desirable to discover the extent to which the function given by equation (12) deviates from the simple cosine function of equation (13) for given circuit constants. This could be done by substituting values for a, b, and Δ, and computing e_{om} from equation (12) point by point. However, aside from requiring laborious calculations, this method is open to the objection that in an actual experimental circuit a, b, and Δ may not be known exactly, but may be defined by limits of variation. This is especially true of Δ, since the two input signals must be matched by comparing meter readings which are subject to a limited but variable error. Thus a means of expressing directly the deviation of the exact output function from the simple cosine function would be very valuable in the application of the theory to actual phase measurements. The required equations are derived as follows:

In equation (12) let the expression under the radical be represented by F. Then

$$e_{om} = e \sqrt{F}$$

where

$$F = 1 + \Delta^2 a^2 - 4(a - a^2 - b^2 - \Delta a^2) \sin^2 \frac{\theta}{2} + 2\Delta a \cos \theta + 2(1 + \Delta) b \sin \theta .$$

We may rewrite the expression for F as

$$F = 1 - \sin^2 \frac{\theta}{2} - 4\left(a - a^2 - b^2 - \Delta a^2 - \frac{1}{4}\right) \sin^2 \frac{\theta}{2} + \Delta^2 a^2 + 2\Delta a \cos \theta + 2(1 + \Delta) b \sin \theta .$$

We now make these definitions

Let
$$M = -4\left(a - a^2 - b^2 - \Delta a^2 - \frac{1}{4}\right)$$

$$(1 + p) = \frac{2\Delta a}{M}$$

$$N = 2(1 + \Delta) b$$

The term $\Delta^2 a^2$, having Δ^2 as a factor, has been found to be negligible for good experimental conditions and will be dropped from the expressions.

Then

$$F = 1 - \sin^2 \frac{\theta}{2} + M \sin^2 \frac{\theta}{2} + M(1 + p) \cos \theta + N \sin \theta .$$

Since

$$1 - \sin^2\frac{\theta}{2} = \cos^2\frac{\theta}{2},$$

and

$$\sin^2\frac{\theta}{2} = \frac{1 - \cos\theta}{2}$$

and we have:

$$F = \cos^2\frac{\theta}{2} + \frac{M(1 - \cos\theta)}{2} + M(1 + P)\cos\theta + N\sin\theta$$

$$F = \cos^2\frac{\theta}{2} + \frac{M}{2} - \frac{M}{2}\cos\theta + M\cos\theta + Mp\cos\theta + N\sin\theta$$

$$F = \cos^2\frac{\theta}{2} + \frac{M}{2}(1 + \cos\theta) + Mp\cos\theta + N\sin\theta.$$

Since

$$\frac{1 + \cos\theta}{2} = \cos^2\frac{\theta}{2}.$$

Then

$$F = \cos^2\frac{\theta}{2} + M\cos^2\frac{\theta}{2} + Mp\cos\theta + N\sin\theta$$

$$F = (1 + M)\left(\cos^2\frac{\theta}{2} + \frac{Mp}{1+M}\cos\theta + \frac{N}{1+M}\sin\theta\right).$$

Substituting this final value of F we have

$$e_{om} = e\sqrt{1 + M}\sqrt{\cos^2\frac{\theta}{2} + \frac{Mp}{1+M}\cos\theta + \frac{N}{1+M}\sin\theta}. \qquad (14)$$

This expression shows that impedance and voltage unbalances may be considered to have two separate effects. In the first place, a constant multiplying factor, $\sqrt{1 + M}$, is introduced. This causes no difficulty where experimental data is to be compared to the theoretical function, since the value of this factor may be easily determined and the data corrected accordingly. The second effect of circuit unbalance is the addition of $\cos\theta$ and $\sin\theta$ terms to the $\cos^2(\theta/2)$ term which represents the theoretical characteristic. The discrepancies due to these terms could be determined by computing the value of e_{om} at a number of points, but if the errors are reasonably small, equation (14) may be used to advantage to compute the deviations directly. The application of this method depends upon the magnitudes of the coefficients $Mp/(1 + M)$ and $N/(1 + M)$ being small compared to unity. For good experimental conditions, this condition will be fulfilled.

For the work done on the subject unit, the following values were computed

$$\frac{Mp}{1+M} = 0.00092$$

$$\frac{N}{1+M} = 0.0030.$$

For these small values, the following approximations may be made:

Let

$$e_{om} = e\ \sqrt{1+M}\ \ \sqrt{D(1+q)}\ ,$$

where

$$D = \cos^2\frac{\theta}{2},\ q = \frac{Mp\cos\theta + N\sin\theta}{(1+M)\cos^2\frac{\theta}{2}}.$$

If $q << 1$,

$$e_{om} = e\ \sqrt{1+M}\ \sqrt{D}\ \ (1+\frac{q}{2})\ , \tag{15}$$

and the percentage error due to q is given by

$$E_p = \frac{q}{2} x\ 100. \tag{16}$$

The actual numerical error is given by $e_{om}\ x\ \frac{q}{2}$ or:

$$E_n = e\ \sqrt{1+M}\ \cos\frac{\theta}{2} x\ \frac{Mp\cos\theta + N\sin\theta}{2(1+M)\cos^2\frac{\theta}{2}}\ ,$$

(Since $e_{om} = e\ \sqrt{1+M}\ \cos\frac{\theta}{2}$, very nearly)

and

$$E_n = \frac{e(Mp\cos\theta + N\sin\theta)}{2\ \sqrt{1+M}\ \cos\frac{\theta}{2}}\ . \tag{17}$$

If we wish to determine the phase error caused by a small error E_N in e_{om}, we may simply divide E_N by the derivative of with respect to θ at the point in question

$$E_\theta = \frac{E_N}{\frac{de_{om}}{d\theta}} \tag{18}$$

Since

$$e_{om} = e\sqrt{1+M}\cos\frac{\theta}{2}$$

to a close approximation,

$$\frac{de_{om}}{d\theta} = e\sqrt{1+M}\left(-\sin\frac{\theta}{2}\right)\left(\frac{1}{2}\right)$$

and

$$E_\theta = \frac{e\,(Mp\cos\theta + N\sin\theta)}{e\,(1+M)\left(\frac{1}{2}\right)\left(-2\cos\frac{\theta}{2}\sin\frac{\theta}{2}\right)}$$

or since

$$2\cos\frac{\theta}{2}\sin\frac{\theta}{2} = \sin\theta$$

$$E_\theta = \frac{Mp\cos\theta + N\sin\theta}{(1+M)(-\sin\theta)\left(\frac{1}{2}\right)} = \frac{-2\,Mp}{(1+M)}\cot\theta - \frac{2N}{(1+M)}\,. \tag{19}$$

Because of the approximation made in deriving the equations for E_N and E_θ they must be used with some care. At $\theta = \pi$ the product $D(1+q)$ in the original equation for e_{om} reduces to the indeterminate form $0 \times \infty$ as q approaches ∞ and the method fails, but for any value of θ between 0° and 170°, q remains small and the approximation is very good. For example, at $\theta = 170^\circ$, $q = 0.183$. The approximation made in the derivation was the substitution of the quantity $1 + q/2$ for $\sqrt{1+q}$.

Here we have

$$\sqrt{1+q} = \sqrt{1.183} = 1.087$$

$$\left(1+\frac{q}{2}\right) = 1 + \frac{0.183}{2} = 1.091.$$

Thus the actual error has 0.087 as a factor while the approximation gives 0.091, or a difference of 4.6% of the error itself. For values of θ smaller than 170°, the discrepancy becomes much smaller.

Examination of the equation (19) defining E_θ discloses that no function of θ has the constant N as a coefficient. This indicates that for small values of N the only error introduced is a constant displacement of the curve for e_{om} from the basic $\cos(\theta/2)$ curve. Since N is dependent on b, the imaginary component of the impedance ratio $Z_1/(Z_1 + Z_2)$, this means that small differences in phase between the driving impedances of the bridge cause negligible distortion of the phase characteristic.

Experimental Procedure

The experimental setup used in the calibration of the subject unit is illustrated in Figures 7 and 8. The i-f amplifiers used were two identical synchronous-tuned strips designed for 30-Mc i-f work where phase stability was important. The construction of the mixer is not especially critical. If good r-f practice is folfowed, no difficulty should be experienced. The 120-ohm resistors employed in the mixing network provide approximate terminations of the 72-ohm cables to the amplifiers, and are sufficiently low in value to make stray capacity unbalance unimportant without causing excessive loading of the amplifier outputs. The 12K series resistor and 30-Mc tuned circuit were found adequate to reduce the harmonic content at the detector to a negligible percentage. The effective generator impedances, Z_1 and Z_2, were determined experimentally by means of an r-f bridge. The input resistor connections at point (A), Figure 8, were broken and the impedances to ground were measured at these two points with the i-f strips connected. Measurements were made with and without supply voltages applied to the amplifiers, and negligible variations were observed at the gain settings employed. The input voltages were matched during calibration runs by comparing output readings with the supply voltage removed from each strip in succession.

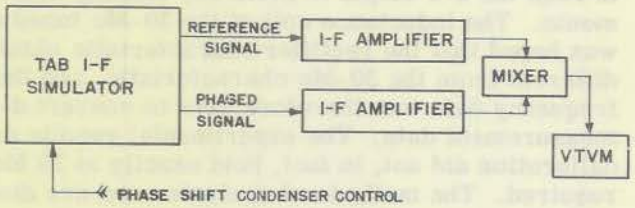

Figure 7 - Phase calibration setup

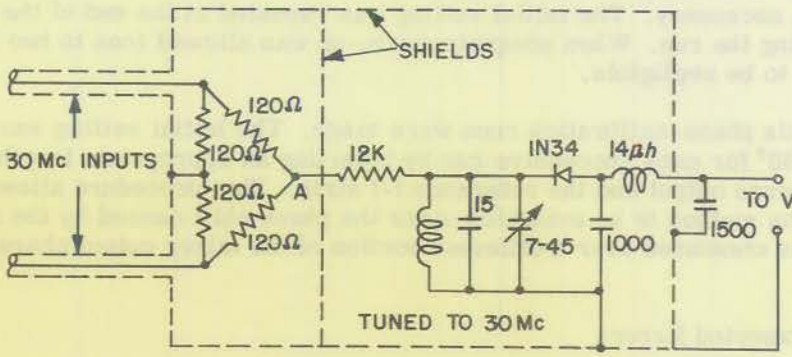

Figure 8 - Mixer details

The accurate measurement of the output voltage from the mixer is perhaps the most difficult experimental problem in the application of this phase measurement technique. To secure results accurate enough to be useful in this application, the output must be measured with a linearity of ± 1% or better, although absolute voltage accuracy is not important. One possibility would be the direct use of a VTVM having an r-f probe, but the best such unit available had a specified accuracy of only ± 3% for a one-volt deflection at 30 Mc. It was therefore decided to employ a calibrated crystal rectifier and d-c VTVM combination. The VTVM was standardized by comparison with an accurate laboratory meter, and the rectifier was calibrated with meters of comparable accuracy.

Because of the low output voltages to be measured (one volt of rectified dc at maximum mixer output), the characteristic of the crystal was nonlinear over a large part of the desired operating range and accurate calibration data was essential. Calibration was performed at 5 kc using a sinusoidal signal of low harmonic content from a good audio oscillator. During calibration the r-f bypasses of the rectifier were shunted by audio bypasses to preserve the same rectification efficiency, and a standardized VTVM employed to read the d-c output to avoid any loading which would not be present during r-f measurements. The inductance coil of the 30-Mc tuned circuit was, of course, disconnected. It was hoped that the rectifier characteristic obtained by this method would not be appreciably different from the 30-Mc characteristic, and the correction curve plotted from the low-frequency data was therefore used to convert d-c output to ac in analyzing the phase-measurement data. The experimental results demonstrated later that the low-frequency calibration did not, in fact, hold exactly at 30 Mc, and further correction of the data was required. The methods of analysis used are discussed in a following section.

In making a phase-calibration run the equipment shown in Figure 4 was assembled and all units allowed to warm up for at least two hours. Switches were provided which enabled the B-supply voltage to be removed from one i-f strip momentarily without disturbing the operation of the other. To start a run, the phase-shift dial of the unit was set to the reading which yielded the minimum mixer output when the two input signals had been properly matched. Matching was accomplished by observing the output-meter deflections when the plate supply to each strip was momentarily switched off. If the two i-f outputs were not matched, the input levels were adjusted until a balance was obtained. This input level was then maintained during the entire run. The minimum mixer output at the initial phase setting is theoretically zero and in practice was too small to cause any readable deflection of the output meter. After the initial setting had been established, the run was completed by recording the output-meter readings at the ten-degree points around the dial, rechecking the input-signal balance before each reading, and adjusting the levels when necessary. The initial setting was repeated at the end of the run to check phase drift during the run. When adequate warm-up was allowed (one to two hours), this drift was found to be negligible.

A total of six phase-calibration runs were made. The initial setting was shifted by approximately 60° for each successive run by inserting an appropriate length of cable between the reference output and the reference i-f strip. This procedure allows inaccuracies of the calibration method to be evaluated since the phase shift caused by the same change in dial setting is measured over a different portion of the mixer output characteristic for each run.

Evaluation of Expected Errors

The experimental problems encountered in the use of this phase-calibration method are those of accurate voltage amplitude measurement, and meter calibration is therefore of great importance. In calibrating the crystal rectifier at 5 kc, the VTVM used to measure

the d-c output was standardized within ± 0.75% of full scale and the meter measuring a-c input was calibrated within ± 0.5% of full scale. The line voltage supplying the meters was held constant within close limits, but the small variations permitted added ± 0.2% to the error of the d-c meter and ± 0.1% to that of the a-c meter. The over-all reliability of the rectifier calibration data is thus ± 1.28% where the d-c output is one volt (approximately full scale deflection for both meters), and becomes poorer at lower outputs. The a-c meter was switched to a lower scale for low readings so that its accuracy of reading was maintained at ± 1.5% or better. The d-c meter, however, had only a one-volt scale and its percentage accuracy was thus proportional to the deflection. The maximum error under any condition may be expressed as

$$\text{Max. Error} = \pm 1.5\% \pm \frac{0.75\%}{D}, \tag{20}$$

where D is the d-c meter deflection expressed as a fraction of full scale.

The output meter used for the phase-calibration runs was the same one used in determining the rectifier characteristic. The precision of this measurement was thus ± 0.75% of full scale, plus any day-to-day drifts in the linearity of VTVM circuit. Recalibration of the meter on several successive days indicated that the uncertainty of calibration was less than ± 0.5% during variation of the ambient temperature over a ± 15° F range. Thus, at worst, the accuracy of output metering was ± 1.25% of full scale.

The phase errors caused by inaccurate metering of the mixer output voltage may be computed as follows. For small errors, we have Equation 18,

$$E_\theta = \frac{E_N}{\frac{de_{om}}{d\theta}}$$

where E_N is the numerical error of metering and E_θ is the resulting displacement of the curve for e_{om} along the θ-axis. From equation (15):

$$e_{om} = e\sqrt{1+M}\cos\frac{\theta}{2}, \quad \text{(very nearly)}$$

and

$$\frac{de_{om}}{d\theta} = \frac{-e\sqrt{1+M}}{2}\sin\frac{\theta}{2}.$$

Here

$$\sqrt{1+M} = \sqrt{1.048} = 1.024.$$

Substituting we have

$$E_\theta = \frac{E_N}{-0.512e\sin\frac{\theta}{2}},$$

or

$$E_\theta = \frac{-E_N}{e} \times \frac{1.953}{\sin\frac{\theta}{2}} \quad \text{radians.} \tag{21}$$

For the ± 1.25% metering accuracy computed above, we have

$$E_N = \pm\, 0.0125e$$

$$E_\theta = \frac{\mp\, 0.0125 \times 1.953 \times 57.3}{\sin\frac{\theta}{2}}$$

$$E_\theta = \frac{\mp\, 1.40}{\text{Sin}\,\frac{\theta}{2}} \quad \text{degrees.}$$

Typical values of E_θ are

θ	E_θ
10°	∓ 16.1°
30°	5.4°
60°	2.8°
90°	2.0°
120°	1.6°
150°	1.4°
170°	∓ 1.4°

In addition to computation of metering accuracy the extent to which the experimental setup deviates from the ideal is important since it determines the compexity of the computations required to evaluate the data. For the experimental setup used the following impedances were measured:

$$Z_1 = 144 + j8.7 \text{ ohms}$$

$$Z_2 = 151 + j10.0 \text{ ohms.}$$

Thus, where

$$\frac{Z_1}{Z_1 + Z_2} = a - jb,$$

we have

$$a = 0.490$$

$$b = +0.0015.$$

From Equation (19) we have

$$\underset{\text{(radians)}}{E_\theta} = \frac{-2\,Mp}{1+M}\cot\theta - \frac{2N}{1+M},$$

where E_θ is the angular deviation of the output voltage function from a cosine function, M, N, and p are defined by the relations

$$M = -4\left(a - a^2 - b^2 - \Delta a^2 - \frac{1}{4}\right)$$

$$N = 2(1+\Delta)b$$

$$(1+p) = \frac{2\Delta a}{M}$$

and Δ is in turn defined by the equation

$$\frac{e_2}{e_1} = (1+\Delta).$$

From the experimental conditions under which e_1 and e_2 were balanced we have

$$\frac{e_2 Z_1}{e_1 Z_2} = 1, \text{ and } \frac{e_2}{e_1} = \frac{Z_2}{Z_1}$$

since

$$\frac{e_2}{e_1} = \frac{151}{144} = 1.05 \quad \text{very nearly,}$$

$$(1+\Delta) = 1.05 \text{ and } \Delta = +0.05.$$

If the given numerical values of a, b, and Δ are now substituted into the equations for M, N, and p, we find,

$$M = 0.048$$

$$N = 0.0032$$

$$p = 0.020$$

and

$$\frac{2Mp}{(1+M)} = 0.00183, \qquad \frac{2N}{(1+M)} = 0.061.$$

Expressing E_θ in degrees rather than radians, we have

$$E_\theta = 0.00183 \times 57.3 \cot \theta - 0.061 \times 57.3$$

$$E_\theta = 0.105 \cot \theta - 0.349 \text{ degrees.}$$

Values of E_θ for several values of θ are

θ	E_θ (Degrees)
10°	-0.945
30°	-0.531
60°	-0.410
90°	-0.349
120°	-0.288
150°	-0.167
170°	+0.247

It should be noted that the mixer output is a minimum when $\theta = 180^\circ$ which corresponds to phase opposition of the two inputs. Thus, the smallest values of E_θ correspond to small output meter deflections.

If the values for rectifier calibration error are substituted for E_N in equation (21), the phase error contributed by this source may be evaluated. The errors computed in this way are tabulated together with those due to metering inaccuracy and mixer unbalance.

θ	Mixer Unbalance	Output Meter Calibration	Rectifier Calibration
10°	-0.945°	∓ 16.1°	∓ 30.5°
30°	-0.531°	5.4°	10.0°
60°	-0.410°	2.8°	4.8°
90°	-0.349°	2.0°	3.0°
120°	-0.288°	1.6°	2.0°
150°	-0.167°	1.4°	1.7°
170°	+0.247°	∓ 1.4°	∓ 2.0°

It will be seen that the errors caused by the deviation of the mixer circuit from the ideal condition of balance are over five times as small as those which may result because of possible inaccuracy in output meter and rectifier calibration. Consequently, the mixer output will be considered, for purposes of data analysis, to follow the simple $\cos(\theta/2)$ function.

It should be noted that the error figures tabulated are in each case the maximum values that would ever be expected. Actual experimental errors should fall well within these limits. Further, a large part of the error contributed by inaccurate output meter calibration will remain fixed from day to day.

The rectifier calibration is entirely fixed since the same correction curve is used to adjust each set of data. Under the least favorable circumstances, the unpredictable variations in output meter linearity should be not more than one-half of the figures tabulated above. This is the amount of variation which should be expected from one experimental run to the next. These figures are tabulated below

θ	Maximum Variable Phase Error
10^0	$\mp 8.1^0$
30^0	2.7^0
60^0	1.0^0
90^0	0.8^0
120^0	0.7^0
170^0	$\mp 0.7^0$

It should also be mentioned that the error tables above do not include the error due to deviation of the rectifier characteristic at 30 Mc from that at 5 kc. This error would be constant from run to run, but was not found to be negligible when experimental data were analyzed.

Analysis of Data

It was estimated that the maximum output phase error of the phase-shift condenser would be $\pm 4.7^0$ or less if:

(1) The initial values of the bridge arm components are matched within 0.5%, and and the subsequent changes in value due to ambient temperature changes or aging are not greater than an additional 0.5%.

(2) The amplitudes of the driving voltages are matched within 3%.

(3) The driving voltages differ from 180^0 phase opposition by less than 1.0^0.

In aligning the phase-condenser input circuit prior to phase calibration, the bridge-arm components were matched by means of bridge measurements before being installed in the unit. Final adjustment was then made by adjusting the coupling slugs of the transformer and the balancing inductances L_4 and L_5 for the condition of least output amplitude fluctuation. (See Figure 3.) For the best condition of adjustment the observed fluctuation was ± 4%. For this alignment technique, the errors contributed by phase and amplitude errors of the driving voltages should be reduced to the same order of magnitude as those due to bridge inaccuracies. Thus, the three conditions listed above are effectively established and a maximum possible output phase error of $\pm 4.7^0$ would be expected. Since the figure of 4.7^0 applies only in the case of the worst combination of errors, a smaller deviation is probable.

When the phase errors computed for the different experimental runs were compared, the error figures for given phase dial settings were found to differ by as much as 9^0. Run-to-run differences of 7^0 occurred at a number of points around the dial. The error values used for comparison were read from smoothed curves drawn for each run of data. Data for $\theta \leq 10^0$, where the slope of the output voltage function was low and the chance for angular error greater, were given correspondingly little weight. Discrepancies in error value of the order noted could conceivably be accounted for by the output meter and rectifier

calibration errors as tabulated. However, a large number of unfavorable coincidences would have to be assumed to account for all the large differences noted. Further, inspection of the error plots indicate that consistent distortions of the error data occur in each run following the dial readings which correspond to $\theta = 180^{\circ}$, the minimum mixer output. These distortions take the form of a rapid increase in positive dial error as θ decreases and dial readings increase. An increase in error of about $+5^{\circ}$ takes place between $\theta = 180^{\circ}$ and $\theta = 135^{\circ}$ in every run. For these values of θ, the predicted error due to meter and rectifier calibration has a maximum value of only 3.4° if the errors from the two sources happen to add directly. Thus, it seems very likely that another source of nonlinearity is present.

The most logical assumption to make is that the rectifier calibration made at low frequency was not accurate at 30 Mc. Reasoning back from a phase error value of 5° shows that a 4% difference between 5-kc and 30-Mc characteristics at low signal levels (under 0.5 v rectified output) would account for the discrepancy. A possible explanation for the calibration error is nonlinear loading of the 30-Mc tuned circuit by the crystal. No attempt was made to replace this tuned circuit with a 5-kc analog during low-frequency measurement so that this exact loading was not taken into account. Since crystal loading decreases as signal level decreases, nonlinearity would cause an error of the proper sign to appear. Q-meter measurements were made to compare the loading of a crystal rectifier with that of a resistor which was equivalent to the rectifier at high signal levels. When the 30-Mc voltage developed across the tuned circuit was reduced to 1.1 v rms., the rectifier loading was found to be 15% lower than that of the equivalent resistor. This is found to represent a 1.4% error in the output-voltage calibration of the mixer circuit described in this report. Since signal levels much lower than 1.1 volts were encountered during phase measurement it is entirely possible that this effect could account for the observed error.

In order to increase the usefulness of the phase-error data it was decided to attempt an approximate correction of the output-voltage error. By comparing the error curves for the different runs, a correction function was obtained in terms of θ, and this function was then used to correct each set of data. The corrected error curves were much more consistent and showed no deviations which had an observable correlation with the mixer phase angle, θ. A maximum error spread of about 8° was still obtained; but this maximum occurred at only one point on the phase-condenser dial when all data were referred to the same dial zero setting, whereas the uncorrected data exhibited a spread of 8° at a number of erratically spaced dial readings. A polar plot of the corrected error data is given in Figure 9, the width of the outlined band indicating the spread of the data at a particular dial setting. If the average of the spread is taken as the phase error, the maximum errors are approximately $+6^{\circ}$, -0°, or $\pm 3^{\circ}$. This figure is within the predicted range of errors, but more consistent data would be required before $\pm 3^{\circ}$ accuracy could be specified definitely for the phase-shift condenser. The desired data was later obtained by another method of phase calibration. The output amplitude characteristic which the phase-shift condenser exhibited during phase calibration is also plotted in Figure 9. The maximum excursions are $\pm$ 4%.

The Multiplier Method of Phase Calibration

When the mixer data discussed above proved to be unsatisfactory, the use of frequency multiplication to reduce the contribution of mixer and detector circuits to calibration error was proposed.

A system was devised in which the 30-Mc signals were heterodyned to about 1.11 Mc by a common local oscillator and then multiplied eighteen times to 20 Mc for phase comparison. Thus, eighteen sharp nulls were obtained for one cycle of 30-Mc phase shift.

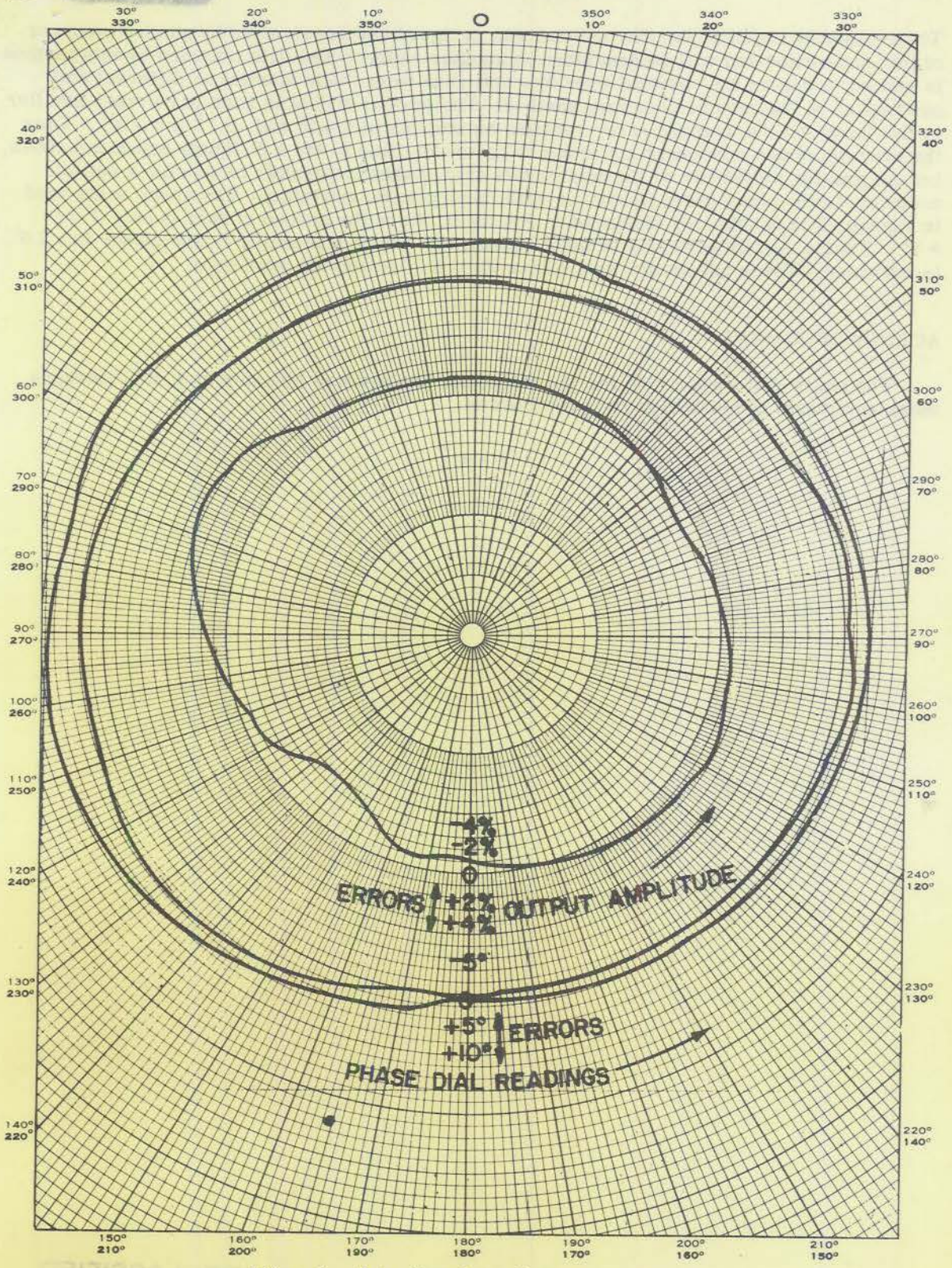

Figure 9 - Data for mixer phase measurements

The equipment required for this method was designed and constructed by another member of this subsection and will be described in another report. The data obtained by this method is plotted in Figure 10. Several experimental runs were made starting at different dial settings as in the case of the mixer method. The spread of data is seen to be much smaller in this case and the average error reaches maximums of $+ 4.5^{\circ}$ and -0.7° or $\pm 2.6^{\circ}$. Thus the over-all phase-condenser accuracy indicated is close to the $\pm 3^{\circ}$ figure estimated above, but the greater reliability of the data in this case makes it possible to ascribe a definite accuracy to the phase-shift condenser with much greater certainty. The error scale used in Figure 10 is double that employed in Figure 9. Here the spread of data is only 2° or $\pm 1^{\circ}$. Thus a certain accuracy of better than $\pm 3.5^{\circ}$, with a probable figure closer to $\pm 2.6^{\circ}$, is indicated. These values are well within the $\pm 4.7^{\circ}$ estimated maximum.

ACKNOWLEDGMENT

The phase calibration data for the multiplier method was obtained by J. H. Campagna using equipment of his design and construction.

* * *

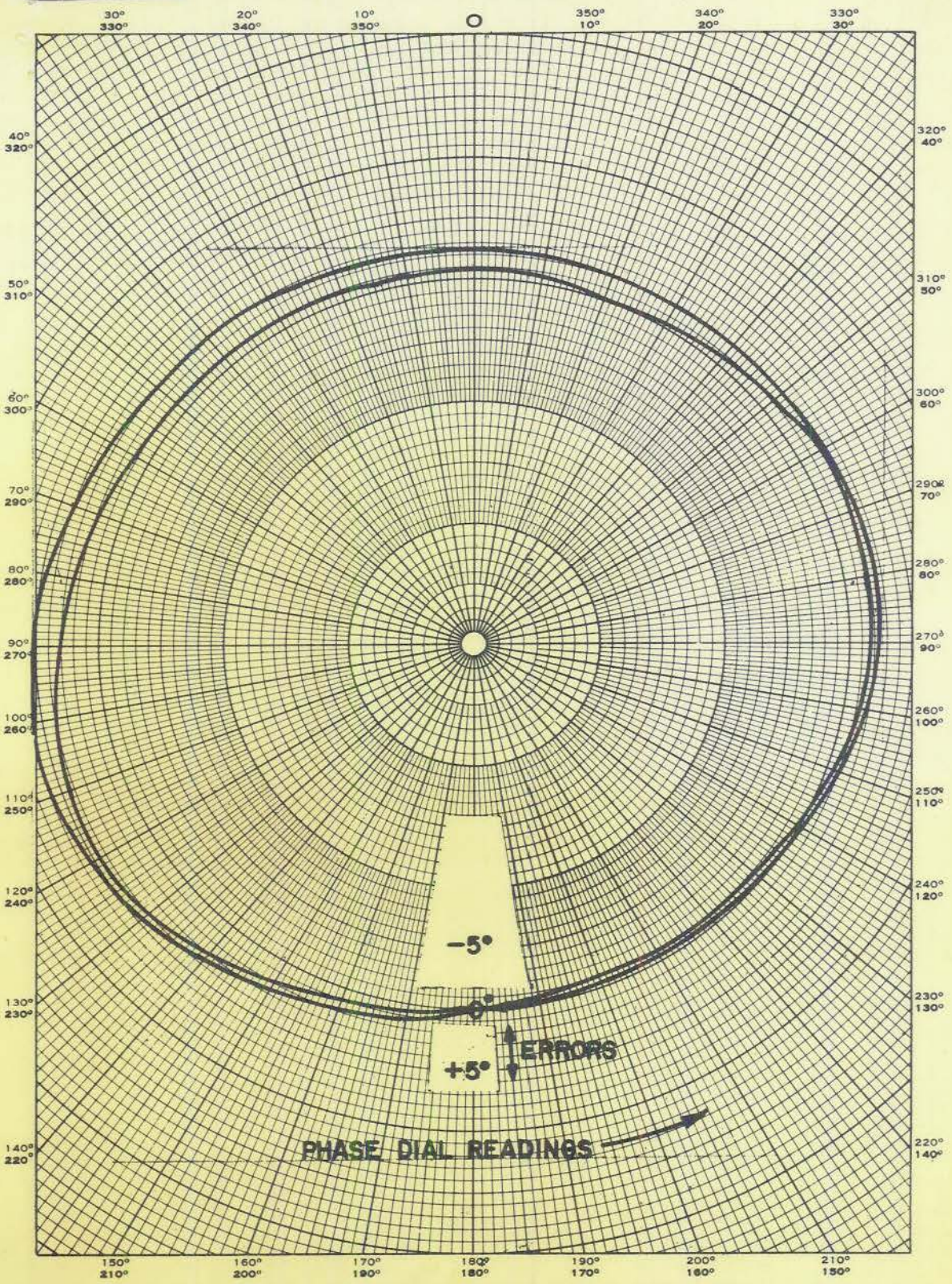

Figure 10 - Data for multiplier phase measurements

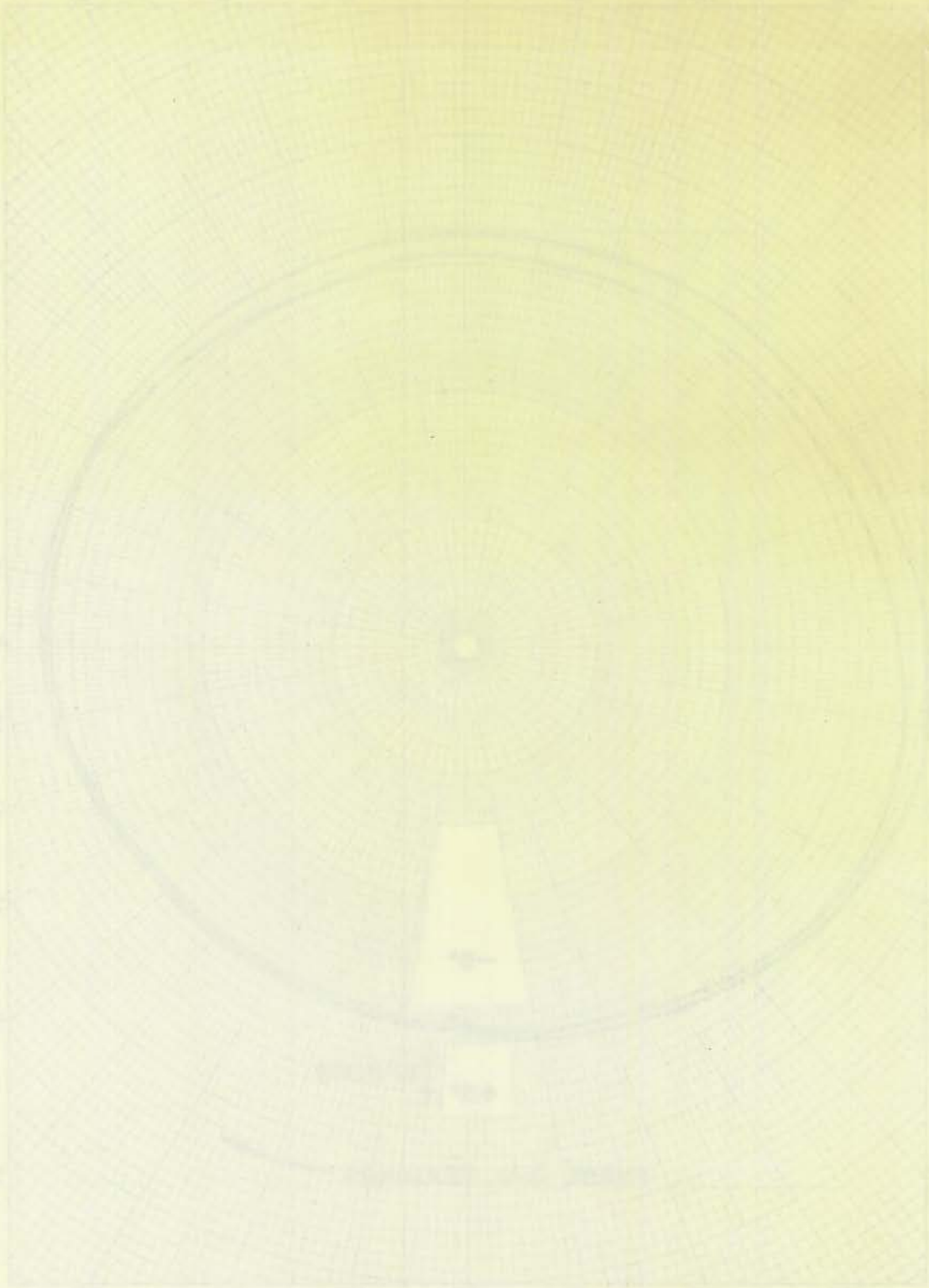

APPENDIX I - CATHODE FEEDBACK EFFECTS

DERIVATIONS

Modification of Input Admittance

NOTE: The plate-cathode and plate-grid capacitances are assumed to be negligible so far as the following derivation is concerned:

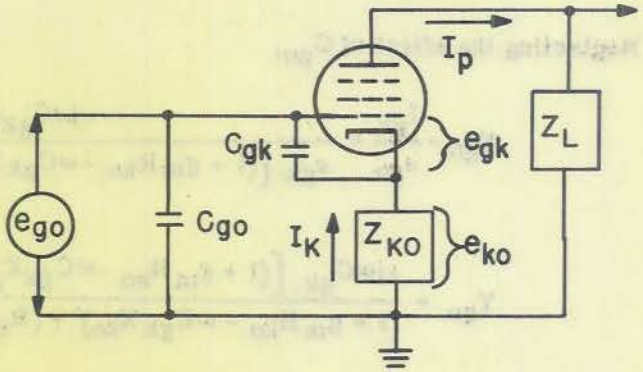

Figure 11 - Pentode amplifier stage with cathode feedback

Using the terminology of Figure 11 we have

$$e_{gk} = e_{go} - I_k Z_{ko}$$

but

$$I_k = I_p + I_{gk}$$

$$I_k = e_{gk} g_m + I_{gk}$$

and

$$e_{gk} = e_{go} - Z_{ko} (e_{gk} g_m + I_{gk})$$

$$e_{gk} (1 + g_m Z_{ko}) = e_{go} - I_{gk} Z_{ko}$$

where

$$I_{gk} = \frac{e_{gk}}{-jX_{gk}} = + j e_{gk} \omega C_{gk}$$

Then

$$e_{gk}\,(1 + g_m Z_{ko}) = e_{go} - j e_{gk}\,(\omega C_{gk})\,Z_{ko}$$

$$e_{gk}\,\left[1 + g_m\,(R_{ko} + jX_{ko}) + j\omega C_{gk}\,(R_{ko} + jX_{ko})\right] = e_{go}$$

$$e_{gk}\,\left[(1 + g_m R_{ko} - \omega C_{gk} X_{ko}) + j(\omega C_{gk} R_{ko} + g_m X_{ko})\right] = e_{go}\,.$$

Neglecting the effect of C_{go},

$$Y_{go} = \frac{I_{gk}}{e_{go}} = \frac{+ j\omega C_{gk} e_{gk}}{e_{gk}\,\left[(1 + g_m R_{ko} - \omega C_{gk} X_{ko}) + j(\omega C_{gk} R_{ko} + g_m X_{ko})\right]}$$

$$Y_{go} = \frac{+j\omega C_{gk}\,\left[(1 + g_m R_{ko} - \omega C_{gk} X_{ko}) - j(\omega C_{gk} R_{ko} + g_m X_{ko})\right]}{(1 + g_m R_{ko} - \omega C_{gk} X_{ko})^2 + (R_{ko}\omega C_{gk} + g_m X_{ko})^2}$$

$$Y_{go} = \frac{(\omega^2 C_{gk}^2 R_{ko} + \omega C_{gk} g_m X_{ko}) + j\omega C_{gk}(1 + g_m R_{ko} - \omega C_{gk} X_{ko})}{(1 + g_m R_{ko} - \omega C_{gk} X_{ko})^2 + (\omega C_{gk} R_{ko} + g_m X_{ko})^2}\,. \qquad (22)$$

For the case of a tube having a bypassed cathode, the resistive component of Z_{ko} will be negligible compared to the reactance at radar i-f frequencies and we may let $R_{ko} = 0$ and $X_{ko} = \omega L_{ko}$. Making these substitutions we have:

$$Y_{go} = \frac{\omega^2 C_{gk} g_m L_{ko} + j\omega C_{gk}\,(1 - \omega^2 C_{gk} L_{ko})}{(1 - \omega^2 C_{gk} L_{ko})^2 + (g_m \omega L_{ko})^2} \qquad (23)$$

$$G_{go} = \frac{\omega^2 C_{gk} g_m L_{ko}}{(1 - \omega^2 C_{gk} L_{ko})^2 + (g_m \omega L_{ko})^2} \qquad (24)$$

$$G_{go} = \frac{g_m C_{gk}}{L_{ko}\,\left[\left(\frac{1}{\omega L_{ko}} - \omega C_{gk}\right)^2 + g_m^2\right]} \qquad (25)$$

Excluding the admittance of C_{go},

$$A_{go} = +j\omega C_{gk} \left\{ \frac{(1 - \omega^2 C_{gk} L_{ko})}{\omega^2 L_{ko}^2 \left[\left(\frac{1}{\omega L_{ko}} - \omega C_{gk} \right)^2 + g_m^2 \right]} \right\} \tag{26}$$

Thus, the component of input susceptance due to grid-cathode capacitance is modified by a factor dependent upon cathode-circuit inductance and tube transconductance.

Phase Angle of the Grid-Cathode Signal

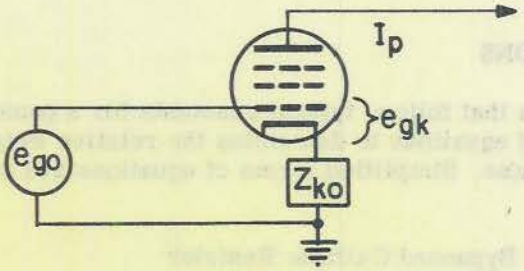

Figure 12 - Simplified pentode circuit for phase angle calculation

In Figure 12

$$e_{gk} = e_{go} - I_p Z_{ko}$$

and

$$I_p = g_m e_{gk}$$

so that

$$e_{gk} = e_{go} - g_m e_{gk} Z_{ko}$$

$$e_{gk} (1 + g_m Z_{ko}) = e_{go}$$

$$\frac{e_{gk}}{e_{go}} = \frac{1}{1 + g_m (R_{ko} + jX_{ko})}$$

Multiplying numerator and denominator by the conjugate of the denominator we have:

$$\frac{e_{gk}}{e_{go}} = \frac{(1 + g_m R_{ko}) - jg_m X_{ko}}{(1 + g_m R_{ko})^2 + (g_m X_{ko})^2} \tag{27}$$

and

$$\theta = \tan^{-1} \frac{-g_m X_{ko}}{1 + g_m R_{ko}} \tag{28}$$

where θ is the angle by which e_{gk} leads e_{go}.

Equation (27) also yields an expression for the complex gain of the stage. By definition:

$$G = \frac{e_{po}}{e_{go}} = \left(\frac{e_{gk}}{e_{go}}\right) \times g_m Z_L .$$

Thus:

$$G = \left[\frac{(1 + g_m R_{ko}) - j g_m X_{ko}}{(1 + g_m R_{ko})^2 + (g_m X_{ko})^2}\right] g_m Z_L . \qquad (29)$$

SAMPLE COMPUTATIONS

In the computations that follow, typical constants for a pentode amplifier stage are substituted into the derived equations to determine the relative weight of the various design factors in a practical case. Simplified forms of equations are presented where their use is indicated.

Input Susceptance for a Bypassed Cathode Resistor

In the equation (26)

$$A_{go} = + j\omega C_{gk} \left\{\frac{(1 - \omega^2 C_{gk} L_{ko})}{\omega^2 L_{ko}^2 \left[\left(\frac{1}{\omega L_{ko}} - \omega C_{gk}\right)^2 + g_m^2\right]}\right\} .$$

Let

$$\omega = 188.5 \times 10^6, \text{ (30 mc/sec.)}$$

$$C_{gk} = 5.5 \times 10^{-12} \text{ farads}$$

$$g_m = .005 \text{ mhos}$$

$$L_{ko} = .01 \text{ microhenries (one-half inch of wire 25 mils in diameter).}$$

Then

$$\omega C_{gk} = 1.038 \times 10^{-3} \text{ mhos}$$

$$\omega L_{ko} = 1.885 \text{ ohms}$$

$$\omega^2 L_{ko}^2 = 3.56$$

$$\omega^2 C_{gk} L_{ko} = 1.957 \times 10^{-3}$$

$$\frac{1}{\omega L_{ko}} = 0.53 \text{ mhos}$$

$$A_{go} = +j1.038 \times 10^{-3} \left[\frac{1 - 0.00196}{3.56\ (0.28 + 25 \times 10^{-6})}\right]$$

$$A_{go} = +j1.038 \times \frac{0.998}{0.996} = +j1.040 \times 10^{-3} \text{ mhos.}$$

Thus the susceptance of C_{gk} is modified only by a factor of 1.002 because of cathode inductance.

Input Susceptance for an Unbypassed Cathode Resistor

Assuming a cathode circuit containing an unbypassed 68-ohm resistor to have the same inductance estimated for the bypassed case the susceptance may be computed from the complete expression for Y_{go} from equation (22) as follows:

$$A_{go} = \frac{+j\omega C_{gk}\,(1 + g_m R_{ko} - \omega^2 C_{gk} L_{ko})}{(1 + g_m R_{ko} - \omega^2 C_{gk} L_{ko})^2 + (\omega C_{gk} R_{ko} + \omega L_{ko} g_m)^2} \qquad (30)$$

$$A_{go} = +j1.038 \times 10^{-3} \left\{\frac{1 + (340 - 2) \times 10^{-3}}{[1 + (340 - 2) \times 10^{-3}]^2 + [(70\ 6 - 9.4) \times 10^{-3}]^2}\right\}$$

$$A_{go} = +j1.038 \times 10^{-3} \left[\frac{1.338}{(1.338)^2 + (0.08)^2}\right]$$

$$A_{go} = +j1.038 \times 10^{-3} \times 0.745$$

$$A_{go} = +j\,(0.996 \times 10^{-3}) \text{ mhos,}$$

and the susceptance of C_{gk} is decreased by a factor of 0.745.

Phase Angle of the Grid-Cathode Signal

For a bypassed or grounded cathode, it was assumed that $R_{ko} = 0$, $X_{ko} = +\ \omega L_{ko}$ = + 1.885 ohms.

Thus in equation (28)

$$\theta = \tan^{-1}\left(\frac{-g_m X_{ko}}{1 + g_m R_{ko}}\right)$$

$$\theta = \tan^{-1}(-.005 \times 1.885) = \tan^{-1}(-.00942)$$

$$\theta = -0.54^{\circ}.$$

For R_{ko} = 68 ohms:

$$\theta = \tan^{-1}\frac{(-.005 \times 1.885)}{1 + .005 \times 68}$$

$$\theta = \tan^{-1}\frac{(-.00942)}{(1.34)} = \tan^{-1}(-.00703)$$

$$\theta = -0.40^{\circ}.$$

Approximate Formulae

The computations made above show that for a tube with a bypassed cathode the ratio between the modified susceptance and that of C_{gk} is very close to unity, and that the term dependent on transconductance has an almost negligible effect. For values of cathode inductance of the order assumed, the expression for A_{go} may be simplified as given below with only a very small error.

$$A_{go} = \frac{+j\omega C_{gk}}{1 - \omega^2 C_{gk} L_{ko}} \quad . \tag{31}$$

This approximation drops the term including g_m and indicates that A_{go} may be regarded as a static quantity unless additional cathode circuit inductance is deliberately inserted. For a tube with an unbypassed cathode resistor, a similar approximation may be made as follows.

$$A_{go} = \frac{+j\omega C_{gk}}{(1 + g_m R_{ko} - \omega^2 C_{gk} L_{ko})} \quad . \tag{32}$$

Here, however, transconductance remains a first-order variable.

Input Conductance for a Bypassed Cathode Resistor

So far as phase stability in the subject unit is concerned, input-conductance variations are a second-order effect. However, the conductance for the circuit constants previously listed is computed as a matter of interest.

For small values of L_{ko} such as are assumed here:

$$G_{go} = \omega^2 C_{gk} L_{ko} g_m, \text{ very nearly.}$$

This form is obtained from equation (22) when the denominator is assumed to be equal to one.

We have:

$$G_{go} = 1.957 \times 10^{-3} \times 5 \times 10^{-3}$$

$$G_{go} = 9.79 \times 10^{-6} \text{ mhos.}$$

This is approximately equivalent to the loading effect of a 100,000-ohm resistor.

DERIVATIVES OF CAPACITANCE FUNCTIONS

In making comparisons of phase stability the derivatives of input capacitance or phase angle with respect to transconductance are the significant quantities.

From equation (32)

$$A_{go} = \frac{+j\omega C_{gk}}{(1 + g_m R_{ko} - \omega^2 C_{gk} L_{ko})} = +j\omega C_{eq}$$

where the equivalent capacitance is C_{eq},

$$C_{eq} = \frac{C_{gk}}{1 + g_m R_{ko} - \omega^2 C_{gk} L_{ko}} .$$

Then

$$\frac{dC_{eq}}{dg_m} = \frac{-C_{gk} R_{ko}}{(1 + g_m R_{ko} - \omega^2 C_{gk} L_{ko})^2} .$$

Actually, $\omega^2 C_{gk} L_{ko}$ is a negligible quantity considering the accuracy to which g_m and R_{ko} are known and,

$$\frac{dC_{eq}}{dg_m} = \frac{-C_{gk} R_{ko}}{(1 + g_m R_{ko})^2} \text{ (very nearly).} \qquad (34)$$

The phase angle by which the voltage leads the current in a single inductor interstage is given by

$$\phi = \tan^{-1} (-R_I \omega C_o) .$$

Then

$$\frac{d\phi}{dC_o} = \frac{1}{1 + (R_I \omega C_o)^2} x\ (-R_I \omega) \tag{35}$$

where R_I is the effective resistive damping of the involved interstage and C_o is the untuned capacitance shunting the inductor. When the interstage is peaked, C_o is theoretically zero and practically will be a fraction of one micromicrofarad. Thus, for application to the low-Q circuits under discussion, equation (35) may be simplified to

$$\frac{d\phi}{dC_o} = (-R_I \omega) = \frac{d\phi}{dC_{eq}} \tag{36}$$

since C_{eq} is a part of the capacity resonated by the interstage inductor.

Thus

$$\frac{d\phi}{dg_m} = \frac{d\phi}{dC_{eq}} \times \frac{dC_{eq}}{dg_m} = \frac{-C_{gk} R_{ko} (-R_I \omega)}{(1 + g_m R_{ko})^2}$$

$$\frac{d\phi}{dg_m} = \frac{+\omega C_{gk} R_{ko} R_I}{(1 + g_m R_{ko})^2}. \tag{37}$$

Substituting the circuit constants as listed

$$\frac{d\phi}{dg_m} = \frac{+1.038 \times 10^{-3} \times 68}{(1 + 0.005 \times 68)^2} \times R_I$$

$$\frac{d\phi}{dg_m} = \frac{+0.071}{1.80} \times R_I = +0.039 R_I \text{ radians/mho}$$

or

$$\frac{d\phi}{dg_m} = +2.25\ R_I \quad \text{degrees/mho.}$$

For R_I = 2700 ohms, which is the value needed to realize a gain of approximately 10,

$$\frac{d\phi}{dg_m} = +6{,}080 \text{ degrees/mho.}$$

This derivative is an indication of the phase stability of the interstage network so far as the effect of cathode feedback on input capacitance is concerned. The positive sign of equation (37) indicates that the voltage developed across the coupling network leads the plate current of the preceding stage by an increasing angle as transconductance increases.

The second cathode effect is the difference in phase between grid-to-ground and grid-cathode signals. This phase angle is given by equation (28),

$$\theta = \tan^{-1}\frac{(-g_m X_{ko})}{(1 + g_m R_{ko})}$$

where a positive angle indicates that the grid-cathode voltage leads the grid-to-ground voltage. Therefore

$$\frac{d\theta}{dg_m} = \frac{1}{1 + \dfrac{g_m^2 X_{ko}^2}{(1 + gmR_{ko})^2}} \left[\frac{(1 + g_m R_{ko})(-X_{ko}) + g_m X_{ko} R_{ko}}{(1 + g_m R_{ko})^2}\right]$$

$$\frac{d\theta}{dg_m} = \frac{-X_{ko}}{(1 + g_m R_{ko})^2 + g_m^2 X_{ko}^2}.$$

If we let $X_{ko} = \omega L_{ko}$,

$$\frac{d\theta}{dg_m} = \frac{-\omega L_{ko}}{(1 + g_m R_{ko})^2 + g_m^2 \omega^2 L_{ko}^2} \qquad (38)$$

$$\frac{d\theta}{dg_m} = \frac{-1.88}{(1 + 0.005 \times 68)^2 + 89 \times 10^{-6}}.$$

In this case, the term $g_m^2 \omega^2 L_{ko}^2$ has a negligible value, and we have

$$\frac{d\theta}{dg_m} = \frac{-\omega L_{ko}}{(1 + g_m R_{ko})^2} \quad \text{(very nearly)}. \qquad (39)$$

Then,

$$\frac{d\theta}{dg_m} = \frac{-1.88}{1.80} = -1.044 \text{ radians/mho}$$

or

$$\frac{d\theta}{dg_m} = -59.8 \text{ degrees/mho.}$$

This effect is thus very much smaller than that of interstage detuning for stages having unity or greater gain.

* * *

APPENDIX II - PHASE INSTABILITY DUE TO MILLER EFFECT

The component of input admittance due to plate-grid feedback in a grounded-cathode stage is given by the equation

$$Y_{go} = Y_{gp}(1 + G). \tag{40}$$

If it is assumed that Y_{gp} is a capacitative reactance, which should be true for a well-constructed stage, we have

$$A_{go} = +j\omega C_{gp}(1 + G)$$

and the equivalent capacitance due to feedback, C_{eq}, is given by

$$C_{eq} = C_{gp}(1 + G). \tag{41}$$

In this equation C_{gp} is the total effective capacity coupling between plate and grid and will be much larger than the tube grid-plate capacitance when an r-f pentode is being considered.

From Appendix I, equation (29),

$$G = \left[\frac{(1 + g_m R_{ko}) - jg_m X_{ko}}{(1 + g_m R_{ko})^2 + (g_m X_{ko})^2}\right] g_m Z_L.$$

Substituting the constants assumed in Appendix I

$$G = \left[\frac{(1 + 0.005\, R_{ko}) - j\,0.0094}{(1 + 0.005\, R_{ko})^2 + 88.7 \times 10^{-6}}\right] g_m Z_L.$$

The imaginary component of G will cause an input conductance to appear even though Y_{gp} is a pure reactance. The phase angle is small, however, about 0.6° at most for the value of X_{ko} assumed, and may be neglected when phase instability is computed. It is also a sufficiently close approximation to assume that $Z_L = R_L$, and the $(g_m X_{ko})^2$ term has a negligible effect.

Making these approximations we have:

$$G \doteq \frac{g_m R_L}{(1 + g_m R_{ko})}, \tag{42}$$

where R_L is the plate load of the stage involved.

It should be noted that this expression becomes inaccurate as does equation (29) when g_m is reduced to the point where the load currents due to grid-plate coupling and other leakage effects become comparable to the tube current. However, with broadband interstages this will occur only at small fractional gains much less than unity and the discrepancy will be negligible at the value of g_m assumed in this discussion.

Substituting in equation (41):

$$C_{eq} = C_{gp}\left(1 + \frac{g_m R_L}{1 + g_m R_{ko}}\right)$$

$$C_{eq} = C_{gp}\left[\frac{1 + g_m(R_{ko} + R_L)}{1 + g_m R_{ko}}\right] \tag{43}$$

$$\frac{dC_{eq}}{dg_m} = \frac{C_{gp}\left[(1 + g_m R_{ko}) R_L - g_m R_L R_{ko}\right]}{(1 + g_m R_{ko})^2}$$

$$\frac{dC_{eq}}{dg_m} = \frac{C_{gp} R_L}{(1 + g_m R_{ko})^2}. \tag{44}$$

Since from Appendix I, equation (36)

$$\frac{d\phi}{dC_{eq}} = (-\omega R_I)$$

we have:

$$\frac{d\phi_{\text{Miller}}}{dg_m} = \frac{-\omega C_{gp} R_I R_L}{(1 + g_m R_{ko})^2}. \tag{45}$$

Substituting the constants of Appendix I, for $g_m R_{ko}$ and ω and assuming $C_{gp} = 0.08\,\mu\mu f$, and $R_I = R_L = 2700\,\Omega$ for a gain of 10:1;

$$\frac{d\phi}{dg_m} = \frac{-188.5 \times 10^{-6} \times 0.08 \times 10^{-12} \times 2700^2}{1 + 0.005 \times 68}$$

$$\frac{d\phi}{dg_m} = \frac{-110}{1.80} = 61.1 \text{ radians/mho}$$

$$\frac{d\phi}{dg_m} = -61.1 \times 57.3 = -3500 \text{ degrees/mho.}$$

It is interesting to note that where two successive stages have identical plate loads, as is often the case, and $R_I = R_L$, equation (45) may be rewritten as

$$\frac{d\phi_{Miller}}{dg_m} = -\omega C_{gp} \left(\frac{R_L}{1 + g_m R_{ko}}\right)^2$$

$$\frac{d\phi_{Miller}}{dg_m} = -\omega C_{gp} \frac{G^2}{g_m^2}. \qquad (46)$$

The last form of the equation shows that when a given stage gain is required, the phase instability due to Miller effect is the same for any combination of R_{ko} and R_L which yields the required gain. However, when the same gain must be obtained at a lower g_m the instability increases as $1/g_m^2$. Thus, the figure of -3500^0/mho computed above, applies to any stage having a gain of 10:1 where $R_I = R_L$, so long as the g_m is maintained at 0.005 mhos. It follows from these considerations that cathode degeneration does not reduce the Miller effect but only offers the possibility of compensation by introducing a second input admittance variation of opposite sign and the correct magnitude.

* * *

APPENDIX III
DERIVATION OF THE OUTPUT VOLTAGE FUNCTION FOR A SIMPLE MIXER

The mixer employed in the phase calibration of the subject unit is represented by Figure 6. Re-presented here.

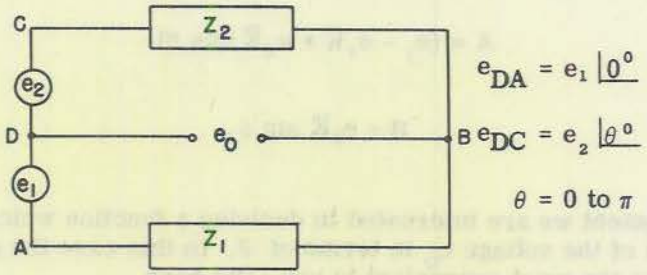

Figure 6 - Balanced mixer

We have:

$$e_o = E_{DB} = E_{DA} + E_{AB} = E_{DA} + I_{AC} Z_1 \cdot$$

But

$$I_{AC} = \frac{E_{AC}}{Z_1 + Z_2} = \frac{E_{AD} + E_{DC}}{Z_1 + Z_2}$$

$$I_{AC} = \frac{-e_1 \angle 0^\circ + e_2 \angle \theta^\circ}{Z_1 + Z_2}$$

$$I_{AC} = \frac{(-e_1 + e_2 \cos\theta + j e_2 \sin\theta)}{Z_1 + Z_2} \cdot$$

Substituting

$$e_o = e_1 + \frac{(-e_1 + e_2 \cos\theta + j e_2 \sin\theta)\, Z_1}{Z_1 + Z_2}$$

let

$$\frac{Z_1}{Z_1 + Z_2} = \bar{K}, \text{ (a complex number).}$$

Then

$$e_o = (e_1 - e_1 \bar{K} + e_2 \bar{K} \cos\theta) + je_2 \bar{K} \sin\theta. \tag{47}$$

The equation for e_o is now in the form A + jB where

$$A = (e_1 - e_1\bar{K} + e_2\bar{K}\cos\theta)$$

$$B = e_2\bar{K}\sin\theta.$$

In this development we are interested in deriving a function which will define the absolute magnitude of the voltage e_o in terms of θ. In this case the polar form of the expression for e_o is the most convenient to use. We have

$$e_o = \sqrt{A^2 + B^2} \; \angle\gamma$$

where A and B are the quantities defined above, and $\gamma = \tan^{-1}(B/A)$. In the present analysis the phase angle of e_o is not significant and we have only to evaluate the quantity $\sqrt{A^2 + B^2}$ which represents magnitude. We have

$$A^2 + B^2 = e_1^2 + 2e_1e_2\bar{K}\cos\theta - 2e_1e_2\bar{K}^2\cos\theta - 2e_1^2\bar{K} + e_1^2\bar{K}^2\cos^2\theta + e_1^2\bar{K}^2 + e_2^2\bar{K}^2\sin^2\theta.$$

$$A^2 + B^2 = e_1^2 + 2e_1e_2\bar{K}\cos\theta - 2e_1e_2\bar{K}^2\cos\theta + e_1^2\bar{K}(\bar{K} - 2) + e_2^2\bar{K}^2.$$

If $e_1 = e_2 = e$, as is the case for balanced input signals,

$$A^2 + B^2 = e^2 \quad [1 + 2\bar{K}(\cos\theta)(1 - \bar{K}) + 2\bar{K}(\bar{K} - 1)]$$

$$A^2 + B^2 = e^2 \quad [1 + 2\bar{K}(1 - \cos\theta)(\bar{K} - 1)]$$

and since

$$(1 - \cos\theta) = 2\sin^2\left(\frac{\theta}{2}\right),$$

$$A^2 + B^2 = e^2 \left[1 - 4\bar{K}(1 - \bar{K})\sin^2\left(\frac{\theta}{2}\right)\right] \tag{48}$$

where $\bar{K} = Z_1/(Z_1 + Z_2)$, as defined above. Where $Z_1 = Z_2$ for a perfectly balanced circuit, $\bar{K} = 1/2 + j\,(0)$ and we have

$$A^2 + B^2 = e^2 \left[1 - \sin^2\left(\frac{\theta}{2}\right)\right]$$

$$A^2 + B^2 = e^2 \cos^2\left(\frac{\theta}{2}\right)$$

and

$$e_{om} = \sqrt{A^2 + B^2} = e \cos\left(\frac{\theta}{2}\right) \tag{49}$$

where e_{om} is the absolute magnitude of the vector voltage e_o.

Thus for matched input voltages and equal driving impedances the output voltage is a simple cosine function. This is, of course, the reason for choosing such a mixer as an experimental device. However, actual experimental circuits will exhibit some unbalance of voltage and impedance, and it is desirable to derive an expression for e_{om} in which the deviation of the function from the basic cosine curve is given in terms of the circuit unbalances. To carry out such a derivation we return to equation (47),

$$e_o = (e_1 - e_1 \bar{K} + e_2 \bar{K} \cos\theta) + je_2 \bar{K} \sin\theta.$$

Now let

$$\bar{K} = \frac{Z_1}{Z_1 + Z_2} = a - jb.$$

Then if $Z_1 = Z_2$, $a = 1/2$ and $b = o$. If $Z_1 \neq Z_2$, a is larger or smaller than $1/2$ and b assumes positive or negative values depending upon the phase angles of the impedances.

Substituting,

$$e_o = e_1 - e_1(a - jb) + e_2(\cos\theta)(a - jb) + je_2(a - jb)\sin\theta.$$

$$e_o = (e_1 - e_1 a + e_2 a \cos\theta + e_2 B \sin\theta) + j(e_1 b - e_2 b \cos\theta + e_2 a \sin\theta).$$

Thus in the form $e_o = A + jB$ we have

$$A = e_1 + e_1 a + e_2 a \cos\theta + e_2 b \sin\theta$$

$$B = e_1 b - e_2 b \cos\theta + e_2 a \sin\theta$$

and $e_{om} = \sqrt{A^2 + B^2}$, as defined earlier.

Squaring and combining terms we have

$$A^2 + B^2 = e_1^2(1 - 2a + a^2 + b^2) + e_2^2(a^2 + b^2) + 2e_1 e_2(a - a^2 - b^2)\cos\theta + 2e_1 e_2 b \sin\theta.$$

To express a voltage unbalance in the mixer circuit, let

$$e_1 = e$$

$$e_2 = e(1 + \Delta).$$

Substituting,

$$A^2 + B^2 = e^2 \left[(1 - 2a + a^2 + b^2) + (1 + 2\Delta + \Delta^2)(a^2 + b^2) + 2(1 + \Delta)(a - a^2 - b^2)\cos\theta + 2(1 + \Delta)b \sin\theta\right]$$

$$A^2 + B^2 = e^2 \left[1 - 2a + 2a^2 + 2b^2 + (2\Delta + \Delta^2)(a^2 + b^2) + 2\Delta(a^2 + b^2)\cos\theta - 2(a^2 + b^2 - a)\cos\theta + 2\Delta a \cos\theta + 2(1 + \Delta)b \sin\theta\right]$$

$$A^2 + B^2 = e^2 \left[1 + 2(1 - \cos\theta)(a^2 + b^2 - a) + 2\Delta(1 - \cos\theta)(a^2 + b^2) + 2\Delta a \cos\theta + \Delta^2(a^2 + b^2) + 2(1 + \Delta)b \sin\theta\right]$$

$$A^2 + B^2 = e^2 \left[1 + \Delta^2(a^2 + b^2) + 4(a - a^2 - b^2)\sin^2\frac{\theta}{2} + 2\Delta a \cos\theta + 4\Delta(a^2 + b^2)\sin^2\frac{\theta}{2} + 2(1 + \Delta)b \sin\theta\right]$$

$$A^2 + B^2 = e^2 \left[1 + \Delta^2(a^2 + b^2) - 4(a - a^2 - b^2 - \Delta a^2 - \Delta b^2)\sin^2\frac{\theta}{2} + 2\Delta a \cos\theta + 2(1 + \Delta)b \sin\theta\right] \quad (50)$$

Equation (50) above is the closest approach that can be made to the form of the simpler equation (48) while retaining all of the terms in the expression. However, in a good experimental circuit, the values of b and Δ will each be much less than 0.1. Under these conditions, terms of the third order or higher, such as $\Delta^2 b^2$, etc. will have negligible magnitude and the second-order terms such as Δb and b^2 will be small.

Dropping third and fourth order terms, we have

$$A^2 + B^2 = e^2 \left[1 + \Delta^2 a^2 - 4(a - a^2 - b^2 - \Delta a^2)\sin^2\frac{\theta}{2} + 2\Delta a \cos\theta + 2(1 + \Delta)b \sin\theta\right] \quad (51)$$

and

$$e_{om} = e\sqrt{1 + \Delta^2 a^2 - 4(a - a^2 - b^2 - \Delta a^2)\sin^2\frac{\theta}{2} + 2\Delta a \cos\theta + 2(1 + \Delta)b \sin\theta}\,. \quad (52)$$

Dropping second order terms we have:

$$A^2 + B^2 = e^2 \left[1 - 4(a - a^2 - \Delta a^2) \sin^2 \frac{\theta}{2} + 2\Delta a \cos\theta + 2b \sin\theta\right]. \qquad (53)$$

$$e_{om} = e \sqrt{1 - 4(a - a^2 - \Delta a^2) \sin^2 \frac{\theta}{2} + 2\Delta a \cos\theta + 2b \sin\theta}. \qquad (54)$$

Further derivations based on equation (52) are carried out in the body of the report in connection with the application of the balanced mixer to phase measurement. Equations 12 to 19 inclusive are pertinent.

* * *